# Chapter 8

# SYNTHESES AND BEHAVIOR STUDIES OF IONIC BONDING DRIVEN UNUSUAL CRYSTAL GROWTH OF ORGANIC AMMONIUM NITRATE SALTS (OANSs)

## Abstract

In this chapter we describe unusual crystal growth of organic ammonium nitrate salts (OANSs). It started with observation of 10 - 15 cm in long white hair-like crystal growth after mixing the aniline with methanolic solution of aluminium nitrate nonahydrate [$Al(NO_3)_3.9H_2O$] as shown in Figure 8.1. SEM images of this white hair-like crystal divulged that it resemble the bamboo structure, in which each shoot is 100 - 200 $\mu$m in length and around 10 $\mu$m in diameter. The white hair-like crystals looks like bamboo trees-like growth. FT-IR, NMR spectra, thermal analyses and powder XRD proved that hair like crystal is nothing but anilinium nitrate (I). In this process we also yielded aluminum oxide ($Al_2O_3$), at the bottom. The SEM and mercury porosimetry analysis on the $Al_2O_3$ confirmed its porous nature with average pore diameter in the 2 - 20 $\mu$m range. The long hair-like crystal growth apparently observed only in protic solvents (alcohol and water) for selected aromatic amines and derivatives. The thermal studies on these OANSs showed endothermic transition while heating and exothermic transition while cooling, a characteristic for solid-solid phase transition. Single crystal XRD analyses on anilinium nitrate-II (sugar-like crystal, prepared by adding dilute $HNO_3$ into the aniline solution in water) reveals that it crystallized in orthorhombic space group *Pbca* with cell dimensions $a$ = 10.158(2) Å, $b$ = 9.277(2) Å, $c$ = 16.177(2) Å, $V$ = 1524.45(5) Å$^3$ and $Z$ = 8. Powder XRD studies showed that anilinium nitrate-I differ from anilinium nitrate-II, polymorphism.

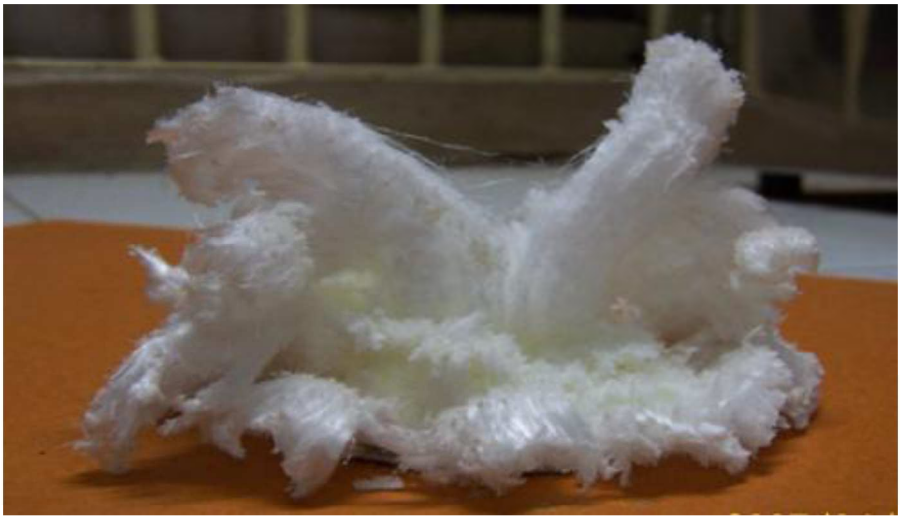

**Figure 8.1** Hair-like crystal growth of anilinium nitrate-I from gel after 8 hours

## 8.1 Introduction

Ammonium nitrate is used as an oxidizer in the propellants, explosives and gas generators. The pure ammonium nitrate has five different solid phases and undergoes four different solid-solid phase transitions before melting. The crystal structure of $NH_4NO_3$ phase-III was determined as orthorhombic structure space group *Pnma* and stable in the range 305 K - 357 K [1,2]. Solid-solid phase transition in ammonium nitrate salts and substituted ammonium nitrate salts have been the subject of numerous recent experimental and theoretical studies. One can prepare mono-, di- and tri-methyl ammonium nitrates by neutralizing the aqueous solution of the corresponding amine with nitric acid. Mono-methyl ammonium nitrate have shown one structural transition at 358 K, whereas tri-methyl ammonium nitrate showed two transitions at 359 K and 409 K [3]. The mono- and di-methyl ammonium nitrates have the explosive properties, while tetra-methyl ammonium nitrate has no explosive properties [4]. The decomposition temperature of these compounds is in the order: $CH_3NH_3NO_3$ > $(CH_3)_2NH_2NO_3$ > $(CH_3)_3NHNO_3$.

Jain *et al.* investigated the thermal stability of ring substituted anilinium nitrate-II [5]. Singh *et al*. have prepared and characterized a large number of ring substituted anilinium nitrate [6]. The full vibrational analyses of anilinium nitrate-II, involving FT-IR, Raman spectra, NMR spectra, SEM measurement, EDAX and crystal structure published in literature [7]. The other nitrate salts such as, hydrazinium nitrate-II exists in two crystalline forms, the stable form melts at 343.7 K while the labile melts at 435.1 K and guanidinium nitrate-II exist as crystal melting at 488 K - 489 K. The significant difference of hydrazinium nitrate-II compared to other nitrate salts is the formation of $NH_3$, which enhances the explosive sensitivity and toxicity [8]. Different orientational disorder caused by rotations and large amplitude librations characterizes the structure [9,10].

Organic ammonium nitrate salts are used in agriculture as a high-nitrogen fertilizer, and in instant cold packs. A number of papers on inorganic and few on organic ammonium salts are available in the literatures [11,12,13,14,15]. Inorganic nitrate salts are well studied for their ferroelectric behavior and reversible structural phase transition [16]. The important as well as often observed structural features in

several of these compounds is N-H···O hydrogen bonding interactions between organic ammonium cations and nitrate anions [17]. N-H···O interaction gives variety of structurally diverse materials. The effect of substituent a methyl group into the ammonium salts in relation to hydrogen bonding is significant [18].

This work deals syntheses, characterization, thermal analysis and single crystal and/or powder XRD studies of OANSs (I and II) and comparison.

## 8.2 Experimental

### 8.2.1 *Materials and methods*

All chemicals and solvents were used of analytical grade reagents. Aniline and benzyl amine (s. d. fine); 4-ethyl aniline, phenyl hydrazine and 4-amino benzoic acid (Fischer scientific, guarated reagent); 4-fluoro aniline (chemport); 4-bromo aniline (sisco research laboratory); 2-methyl aniline, 3-methyl aniline, 4-methyl aniline, 3-fluoro aniline, 4-chloro aniline, (*R*)- and (*S*)-methyl benzyl amine, pyridine, 2-amino pyridine, 3-amino pyridine, 4-amino pyridine and 4-hydroxy pyridine (Aldrich); alcohol and conc. nitric acid (qualigens) were used without any further purification.

### 8.2.2 Syntheses of OANSs

A series (more than fifteen) of OANSs (chiral/non-chiral) were synthesized by using milder synthetic route for nitration, that is by using aluminum (III) nitrate nonahydrate [$Al(NO_3)_3.9H_2O$] and aromatic amines. When aromatic amines [aniline 5.0 mL, 5.11 g (54.869 mmol)] are treated with $Al(NO_3)_3.9H_2O$ [6.861 g (18.290 mmol)] in the ratio of 3:1 in alcohol, a translucent gel obtained. After strong filtration of the gel and its standing for a few hours in open and dry atmosphere, gave hair-like crystal growth of 0.5 - 15 cm long aromatic ammonium nitrate-I salts. The growth of hair-like crystals leaves behind hard cocoon shaped (around 1 - 2 cm long and 0.5 cm thick) particles, which are $Al_2O_3$. We also synthesized the crystal of organic ammonium nitrate-II, by treating a series of aromatic amine (chiral/non-chiral) with concentrated nitric acid ($HNO_3$) in the ratio of 1:1, in alcohol or distilled water. A general methodology of OANSs preparation/syntheses is mentioned in scheme-III.

**Scheme-III**

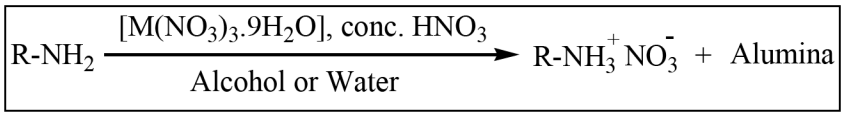


Where, M = Al or Fe and R = $C_6H_5$-, 3-F-$C_6H_4$-, 4-F-$C_6H_4$-, 4-Cl-$C_6H_4$-, 4-Br-$C_6H_4$-, 2-$CH_3$-$C_6H_4$-, 3-$CH_3$-$C_6H_4$-, 4-$CH_3$-$C_6H_4$-, 4-$C_2H_5$-$C_6H_4$-, $C_6H_5CH_2$-, (*R*)-$C_6H_5(CH_3)CH$-, (*S*)-$C_6H_5(CH_3)CH$-, $C_5H_5N$-, 2-$H_2N$-$C_5H_4N$-, 3-$H_2N$-$C_5H_4N$-, 4-$H_2N$-$C_5H_4N$-, $C_6H_4NH$-, etc.

Yield: 10 - 20 % for hair like crystals and 85 - 95 % for sugar like crystals.

The formation of organic ammonium nitrate salts by different routes was confirmed by infrared spectroscopy, $^1$H NMR, thermal analyses and single crystal and/or powder XRD. The formation of alumina were confirmed by powder XRD and solid state $^{27}$Al NMR.

## 8.3 Results and Discussions

### 8.3.1 General Discussion

We observed long hair-like crystal growth for *para*-substituted aniline derivatives. But in case of *meta*- and *ortho*-substitution we observed smaller size of hair-like crystal (or not observed) this means *meta*- and *ortho*-substitution makes growth hindered due to steric reasons. The growth was also observed for pyridine and derivatives, but not for pyrrole. Surprisingly, in a given set of compounds only electron donating group gave hair-like crystal growth. The hair-like crystal growth only observed in protic solvents e.g. alcohol and water, means we did not observed hair-like crystal in aprotic solvents e.g. ether, benzene, toluene, chloroform, dichloromethane, acetonitrile and DMSO. Interestingly, gels prepared using water as a solvent gave growth of hair-like crystal (anilinium nitrate-I), sugar like crystals (anilinium nitrate-II) and thin plates (anilinium nitrate-III), a case similar to concomitant polymorphism [19]. All these crystals (anilinium nitrate) are monotropic in nature, because anilinium nitrate-I and anilinium nitrate-III are converted to anilinium nitrate-II when recrystallized using different solvents [20]. The hair-like growth also depends upon the rate of evaporation of the solvent. Therefore gels

prepared using methanol grows with much higher density than ethanol, which indicates a kinetically controlled mechanism. Since the reaction is kinetically driven, so we expect strong Lewis acidity provided by the exposed aluminium ions will be uniform [21]. On this basis, probable mechanism for overall growth can occur in two step (a) nitrate ion gets attracted toward the anilinium cation formed in the gel by breaking bonding with aluminium cation (competitive ionic binding), (b) slow crystallization of anilinium nitrate (in bamboo type growth of ~10 $\mu$m). Thus, on this basis of formation of rosette shaped alumina and bamboo type structures of anilinium nitrate can be correlated.

### 8.3.2 FT-IR Spectra

The vibrational measurements for a series of OANSs (I and II) were recorded in the range of 4,000 - 400 $cm^{-1}$. On hydro-nitration of organic amines a broad band appears for almost all the OANSs in the region 3250 - 2600 $cm^{-1}$ indicating formation of nitrate salts. The details of FT-IR spectroscopy for a series of OANSs are given in Table 8.1 and 8.2. The strong broad band for N-H ($-NH_3^+$ group) stretching vibrations were observed in the region 3135 - 2600 $cm^{-1}$ due to the continuous series of overlapping bands, combination bands and overtone bands. However, an intense band around 2618 $cm^{-1}$ can be resolved into two features at 2625 $cm^{-1}$ and 2616 $cm^{-1}$. The feature around 2616 $cm^{-1}$ is assigned to the Fermi resonance processes corresponding to combination bands of N-H ($-NH_3^+$ group) deformation mode and N-H ($-NH_3^+$ group) rocking mode. The vibrations observed around 1650 - 1608 $cm^{-1}$ and 1553 - 1528 $cm^{-1}$ are due to bending and symmetric deformation of N-H ($-NH_3^+$ group), respectively [7]. The combination band around 1075 - 1058 $cm^{-1}$ is due to anti-symmetric N-H ($-NH_3^+$ group) rocking. The bands around 1036 $cm^{-1}$, 826 $cm^{-1}$ and 725 $cm^{-1}$ are assigned asymmetric stretching and out of plane bend for $NO_3^-$ ions. Vibration also observed at 1308 $cm^{-1}$ and 1205 $cm^{-1}$ due to C-N stretching. The other modes which provide the vital information about aromatic C-H out of plane deformation, vibrational bands come between 690 - 900 $cm^{-1}$. One expects two vibrational bands between 770 - 730 $cm^{-1}$ and 710 - 690 $cm^{-1}$ for five adjacent hydrogen atoms, 770 - 735 $cm^{-1}$ for four adjacent hydrogen atoms, 810 - 750 $cm^{-1}$ for three adjacent hydrogen atoms and between 860 - 800 $cm^{-1}$ for two adjacent hydrogen atoms. The other vibration mode for aromatic C-F, C-Cl and C-Br stretching were

observed around 1106 $cm^{-1}$, 635 $cm^{-1}$ and 687 $cm^{-1}$ respectively as seen in Figure 8.2. The weak band observed around 1466 $cm^{-1}$ in the spectrum of methyl substituted anilinium nitrate, benzilinium nitrate and (*R*)- and (*S*)-methyl benzilinium nitrate (I and II). This band indicated the deformation of aliphatic C-H [22]. In case of pyridinium nitrate and amine substituted pyridinium nitrate (I and II), vibrational features observed around 3317 $cm^{-1}$ and 1660 $cm^{-1}$ due to the N-H stretching of $NH_2$ and C=N stretching of ring. The bands at 3440 $cm^{-1}$ and 3266 $cm^{-1}$ for 4-hydroxy pyridinium nitrate-I and phenyl hydrazinium nitrate-I are due to O-H stretching and N-H stretching respectively. The band at 1692 $cm^{-1}$ and 1609 $cm^{-1}$ are also observed for 4-hydroxy pyridinium nitrate-I and phenyl hydrazinium nitrate-I due to C=N stretching and N=N stretching respectively see Figure 8.2.

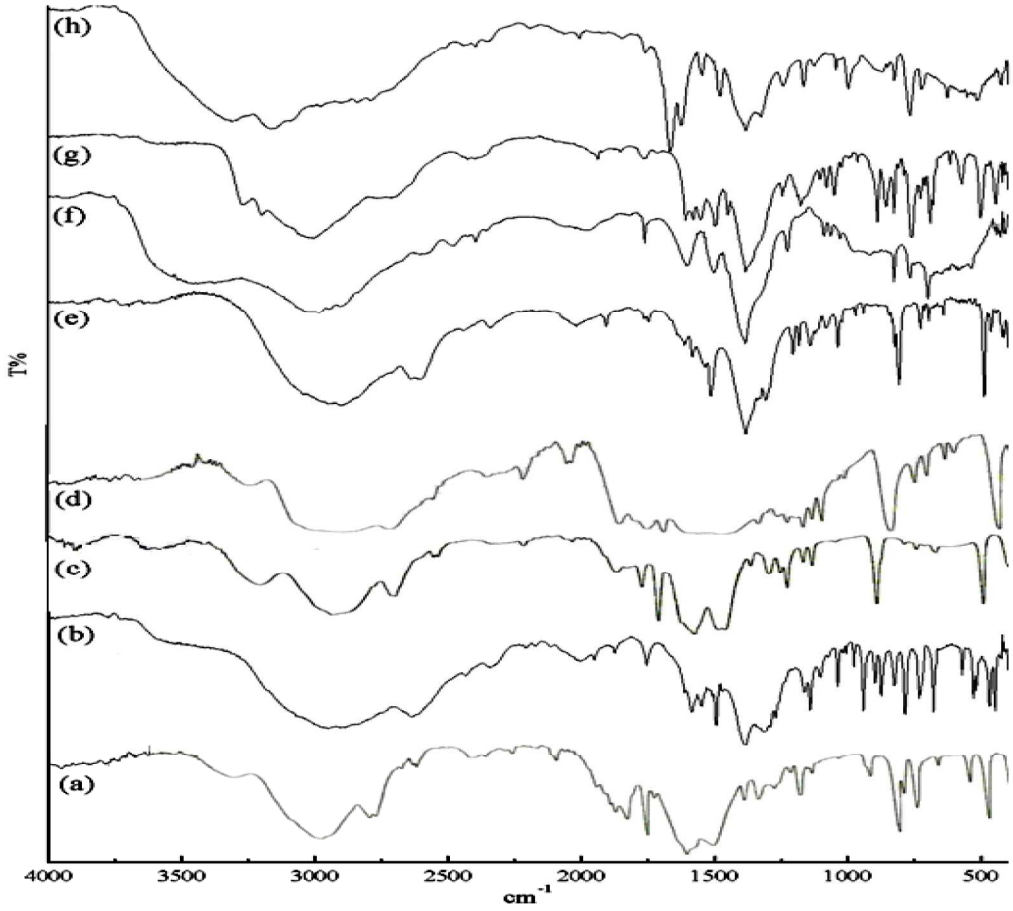


**Figure 8.2** FT-IR spectra of anilinium nitrate-I (a); 3-fluoro anilinium nitrate-I (b); 4-chloro anilinium nitrate-I (c); 4-bromo anilinium nitrate-I (d); 4-methyl anilinium nitrate-I (e); (*S*)-methyl benzilinium nitrate-I (f); 2-amino pyridinium nitrate-I (g) and phenyl hydrazinium nitrate-I (h).

**Table 8.1** FT-IR spectra of organic ammonium nitrate-I, all frequencies are given in $cm^{-1}$

| Compounds | $NH_3^+$ or C-H str. | $^+N$–H···O | $NH_3^+$ def. & rocking | C=C str. | C–H def. | C–N str. & C–C def. | =C-H in plane def. | =C-H out of plane def. | $NO_3^-$ str. & out of plane def. | C–Cl, Br or F str. |
|---|---|---|---|---|---|---|---|---|---|---|
| Anilinium nitrate-I | 2928vs, 2637s | 2065w 1384vs, 961w, 935m | 1638m, 1553s, 1075w | 1602m, 1585m, 1496ssh, 1468m | | 1305vs, 1202m | 1160m, 1058w, 1003w, 994m | 745ssh, 689m | 1036m, 822w, 725m | |
| 4-Fluoro anilinium nitrate-I | 3065vs, 2881vs, 2589s | 2065w, 1396vs, 960w, 936m | 1627m, 1540vssh, 1073w | 1569m, 1500vs | | | 1207w, 1154s, 1021m | 830vs | 1044m, 738s | 1106s |
| 3-Fluoro anilinium nitrate-I | 2950s, 2637s | 2065w, 1384vs, 940s | 1613m, 1548s, 1074w | 1585s, 1494s | | 1309s | 1163m, 1142m, 1006w | 785s | 1038m, 826m, 730m | 1103m |
| 4-Chloro anilinium nitrate-I | 2995vs, 2606s | 2069w, 1385vs, 1291vs, 959w | 1621m, 1542m, 1076w | 1601w, 1493s, 1451m | | 1308vs, 1206m | 1151w, 1115w, 1095m, 1016w | 822s | 1044w, 724w | 635w |
| 4-Bromo anilinium nitrate-I | 2991s, 2882s, 2820vs, 2612s | 2078w, 1386vs, 955w, 936w | 1613w, 1532w, 1070m | 1582w, 1507w, 1485s | | 1331m, 1206m | 1148w, 1116w, 1015m | 812s | 1043m, 726w | 687w |
| 4-Methyl anilinium nitrate-I | 2902s, 2609m | 1383vs, 942w | 1613m, 1536m, 1080m | 1583m, 1514s | 1465m | 1307s, 1205s | 1182m, 1141m, 1021w | 806vs | 1038m, 823s, 725s | |
| 3-Methyl anilinium nitrate-I | 3024s, 2912vs, 2594m | 1375vs, 912w | 1652s, 1528ssh, 1076m | 1596vs, 1496m | 1468w | 1330m, 1201m | 1148m, 1130m, 995m | 779vssh | 1040m, 826s, 721w | |

| | | | | | | | | | |
|---|---|---|---|---|---|---|---|---|---|
| 2-Methyl anilinium nitrate-I | 2904vs, 2870vs, 2605s | 2066w, 1390vs, 944w | 1640s, 1550s, 1076w | 1603s, 1588s, 1500s | 1468w | 1303w | 1162m, 1130m, 999w | 752ssh | 1037s, 823ssh, 726s |
| Benzilinium nitrate-I | 2996vs, 2892s, 2647w | 1385vs, 961w, 921w | 1612m, 1549w, 1079m | 1603m, 1588m, 1513m, 1455m | 1466w | 1308s, 1207s | 1140m, 1104w, 1056w, 997w | 752ssh, 698s | 1030w, 825ssh |
| (*R*)-Methyl benzilinium nitrate-I | 2982vs, 2605m | 2064w, 1397vs, 915m | 1066s | 1604s, 1500s, 1454m | 1475w | 1338w, 1225s | 1175m, 1088s, 1042w | 767s, 699ssh | 1030m, 826ssh, 720w |
| (*S*)-Methyl benzilinium nitrate-I | 3028vs, 2949s, 2904s, 2605m | 2065w, 1385vs, 971w, 917w | 1608m, 1545w, 1080w | 1599m, 1500m, 1453m | 1471w | 1226m | 1191m, 1135w, 1065m, 999m | 767s, 699s | 1030m, 825ssh |
| Pyridinium nitrate-I | 3065vs, 2875s | 2066m, 1383vs, 930m | 1610s, 1537s | 1632s, 1508w, 1487s | | 1338m | 1199m, 1164m, 1093m, | 750s, 679vs | 1048m, 826ssh |
| 3-Amino pyridinium nitrate-I | 3131m, 3059m, 2816m | 2062w, 1385vs | 1633s, 1549vs | 1640s, 1594w, 1504w, 1464w | | 1202w, | 1182w, 1139m, 1008w | 791s | 1344s, 1045m, 826ssh |
| 2-Amino pyridinium nitrate-I | 2165vs, 2978s | 2067w, 1383vs | 1625vs, 1548m, 1075w | 1668vs, 1479s | | 1325s | 1165m, 1126w, 998s | 767s | 1045m, 826m, 723m |
| 4-Hydroxy pyridinium nitrate-I | 3102s, 2967s, 2651m | 1384s, 925w | 1636s, 1538vs, 1090w | 1568w, 1516s, 1451s | | | 1191s, 1138w, 1000m | 830s | 1043w, 726w |
| Phenyl hydrazinium nitrate-I | 3005s, 2717m | 1385vs, 963w | 1551m, 1079m | 1608m, 1580m, 1499s, 1450m | | 1326m | 1176m, 1103w, 1024w, 998w | | 1050m, 826ssh, 726s |

**Table 8.2** FT-IR spectra of organic ammonium nitrate-II, all frequencies are given in $cm^{-1}$

| Compounds | $NH_3^+$ or C-H str. | $^+N$–H···O | $NH_3^+$ def. & rocking | C=C str. | C–H def. | C–N str. & C–C def. | =C-H in plane def. | =C-H out of plane def. | $NO_3^-$ str. & out of plane def. | C–Cl, Br or F str. |
|---|---|---|---|---|---|---|---|---|---|---|
| Ammonium nitrate-II | 3135vs, 3036s, 2802s | 2062w, 1389vs | 1548m, 1074w | | | | | | 1049w, 826ssh | |
| Anilinium nitrate-II | 2934vs, 2638s | 2068w, 1385vs, 960w, 935m | 1638m, 1554s, 1074w | 1602m, 1587m, 1497ssh, 1468m | | 1305vs, 1203m | 1161m, 1058w, 1003s, 994m | 747ssh, 690m | 1038m, 822w, 725m | |
| 4-Fluoro anilinium nitrate-II | 2971s, 2886s, 2638s | 1383vs, 1306s, 960w, 937m | 1610m, 1545m, 1079w | 1597m, 1501s | | 1207m | 1189m, 1157s, 1016m | 830vs | 1045m, 739s | 1112m |
| 3-Fuoro anilinium nitrate-II | 2950vs, 2594s | 1383vs, 941m | 1619s, 1548s, 1072w | 1591s, 1493ssh, 1448w | | 1306w | 1142m, 1094w, 1055w | 783m | | 1109w |
| 4-Chloro anilinium nitrate-II | 2992vs, 2604s | 2065w, 1385vs, 1298vs, 936w | 1623s, 1542s, 1093m | 1584m, 1494s, 1451vs | | 1289vs, 1206m | 1150m, 1117m, 1017s | 821s | 1043w, 732w | 633w |
| 4-Bromo anilinium nitrate-II | 2894s, 2618s | 2076w, 1384vs, 955w, 935w | 1619s, 1534s, 1069s | 1583m, 1487s, 1448s | | 1307vs, 1205m | 1147w, 1116s, 1013s | 809vs | 1042s, 727w | 689w |
| 4-Methyl anilinium nitrate-II | 2917vs, 2581s | 1385vs, 966w, 937m | 1639m, 1548m, 1070w | 1598m, 1579w, 1506vs | 1465w | 1301s, 1205m | 1157s, 1111s, 1017m | 829vs | 1045s, 739m | |

| | | | | | | | | | |
|---|---|---|---|---|---|---|---|---|---|
| 3-Methyl anilinium nitrate-II | 3024s, 2634s | 1378w, 967w, 914ssh | 1640w, 1550m, 1079m | 1606s, 1503w, 1453w | 1467w | 1306w, 1201w | 1153m, 1130m, 998w | 780vssh | 1040m, 824ssh, 725s |
| 2-Methyl anilinium nitrate-II | 2905vs, 2868vs, 2700s, 2604s | 2066m, 1391vs, 946w | 1640m, 1551s, 1065m | 1603w, 1589s, 1500s, 1468w | | 1305w | 1182m, 1162m, 1130m, 1091 | 752vssh | 1036ssh, 823ssh, 727s |
| Benzilinium nitrate-II | 3010vs, 2894s, 2646m | 1385vs, 972s, 920w | 1615s, 1517w, 1058m | 1591s, 1575w, 1505m, 1456m | 1463m | 1306s, 1216s | 1138s, 1103m, 1004w, 995w | 752vssh, 698vssh | 1031m, 824ssh, 718m |
| (*R*)-Methyl benzilinium nitrate-II | 2985m, 2879m | 1382vs, 971w, 935w | 1634vs, 1513s, 1066w | 1579m, 1502s | 1458s | 1227s | 1135w, 1089s, 993w | 768ssh, 698s | 1030w, 831s |
| (*S*)-Methyl benzilinium nitrate-II | 3028vs, 2949s, 2904s, 2605m | 2063w, 1385vs, 934w | 1608m, 1545w, 1065m | 1599m, 1500m, 1453m | 1471w | 1226m | 1188m, 1088m, 1003 | 767s, 699s | 1030m, 825ssh |
| Pyridinium nitrate-II | 3066vs, 2955s 2781vs | 2064w, 1386s, 935w | 1612s, 1536vs, 1055s | 1632s, 1487s | | 1332s | 1200s, 1165s, 1003m | 754vs, 681vs | 1048m, 826ssh, 719w |
| 3-Amino pyridinium nitrate-II | 3065w, 2822w, 2594w | 2068w, 948m | 1641s, 1550vs, 1081w | 1663s, 1571s, 1471m | | 1334s | 1153w, 1118w, 1010m | 801s | 1041m, 824ssh, 718m |
| 2-Amino pyridinium nitrate-II | 3109s, 2788s | 2068w, 1383vs, 972w | 1619s, 1548m, 1066w | 1667vs, 1496w, 1477m | | 1325s | 1165m, 1128w, 1022w | 765vs | 1046m, 826m, 721m |

### 8.3.3 NMR Spectra

$^1$H NMR spectra of anilinium nitrate (I and II) showed broad signal between $\delta$ = 9.79 - 9.89 respectively for three proton due to -$NH_3^+$ moiety, indicates formation of anilinium nitrate salt Figure 8.3 (a) and (b). The signals observed for five proton between $\delta$ = 7.34 - 7.50 are due to the aromatic C-H protons. The peak observed for three proton around $\delta$ = 2.32 for substituted methyl anilinium nitrate salts due to the methyl group on benzene ring. In case of benzilinium nitrate and (*R*)- and (*S*)-methyl benzilinium nitrate peaks around $\delta$ = 4.30 and $\delta$ = 1.48 indicate the benzyl -CH- and $CH_3$ groups protons respectively. The very broad signal (singlet) around $\delta$ = 5.52 and $\delta$ = 13.23 was observed for pyridinium nitrate and amino substituted pyridinium nitrate, indicates hydro-nitration of pyridine ring nitrogen. The observation of signal around the $\delta$ = 5.52 indicates that N-H proton merge with moisture. But in case of amino substituted pyridinium nitrate the broad signal (singlet) are also observed at $\delta$ = 8.01 for 2H proton ($NH_2$) along with $\delta$ = 13.23 conforming mono protonation of the base and amine functionality of pyridine remain unreacted. For 3-amino pyridinium nitrate-II the N-H proton of pyridine was not detected, may be due to the exchange of proton with solvent. In phenyl hydrazinium nitrate-I peaks at $\delta$ = 9.76 and $\delta$ = 8.33 are due to the three and one proton of -$NH_3^+$ and -NH. The details of $^1$H NMR spectra for these OANSs are tabulated in Table 8.3.

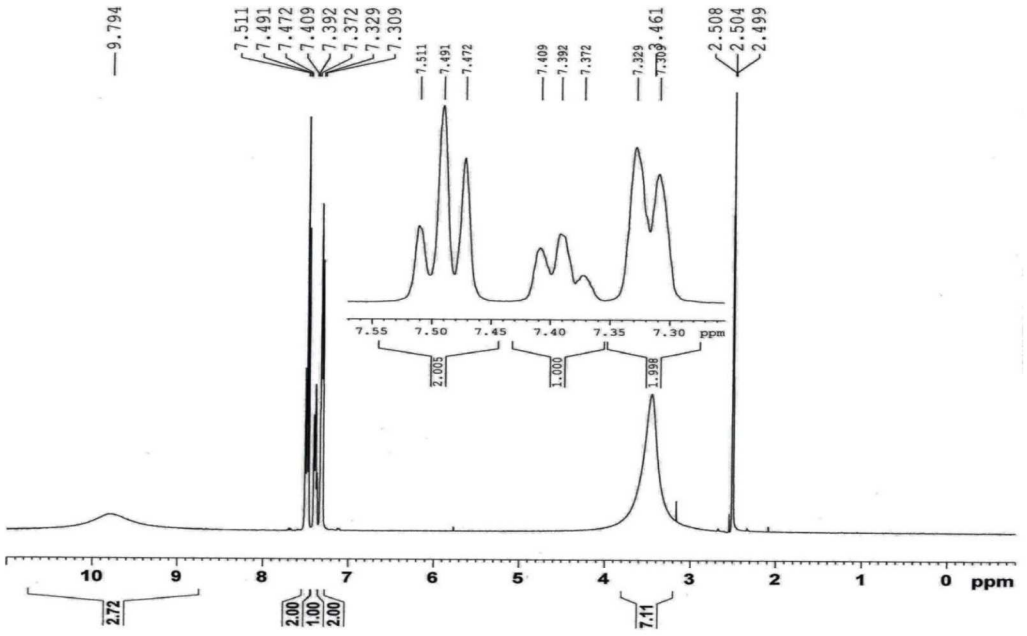


(a)

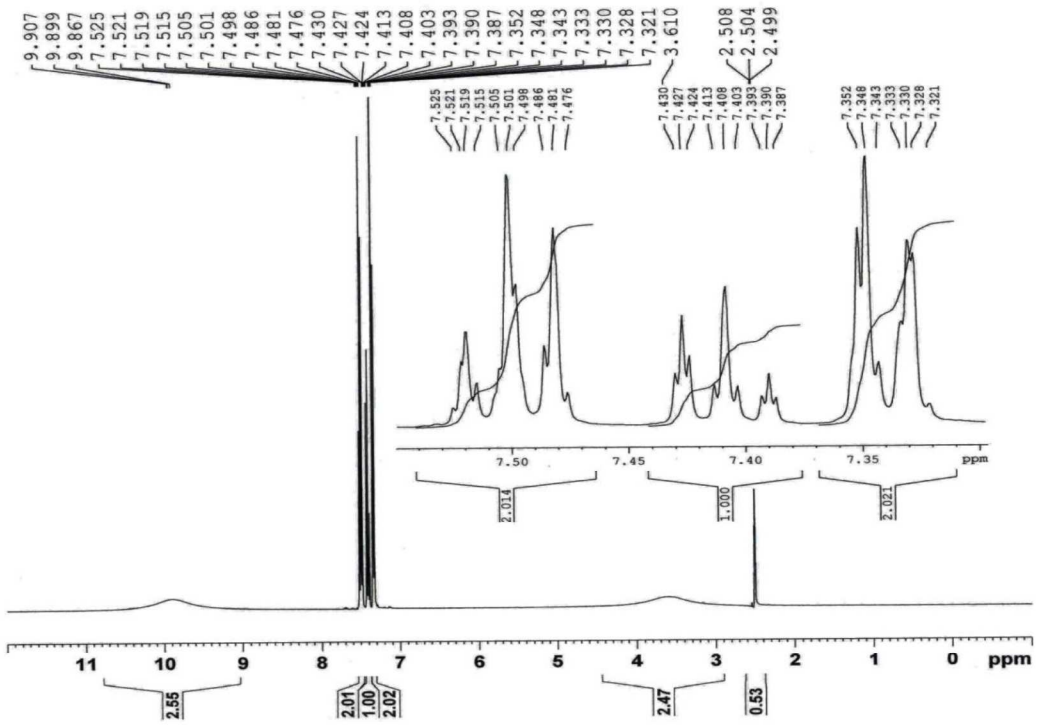


(b)

**Figure 8.3** $^{1}$H NMR spectra of anilinium nitrate-I (a) and anilinium nitrate-II (b).

**Table 8.3** $^{1}$H NMR spectra of OANSs

| **Compounds** | **Gel hair ($\delta$ value) $^{1}$H NMR ($d_6$-DMSO) *J* coupling in Hz** | **Sugar ($\delta$ value) $^{1}$H NMR ($d_6$-DMSO) *J* coupling in Hz** |
|---|---|---|
| Anilinium nitrate | 9.79 (br s 3H, $NH_3^+$), 7.50 (tt 2H, *J* = 6.8 and 8.1), 7.41 (tt 1H, *J* = 7.6 and 7.2), 7.34 (dt 2H, *J* = 6.9) | 9.89 (br s 3H, $NH_3^+$), 7.50 (tt 2H *J* = 6.8 and 8.1), 7.41 (tt 1H, *J* = 7.6 and 7.2), 7.34 (dt 2H, *J* = 6.9) |
| 4-Fluoro anilinium nitrate | 9.79 (br s 3H, $NH_3^+$), 7.32–7.40 (m 4H) | 9.89 (br s 3H, $NH_3^+$), 7.32–7.41 (m 4H) |
| 3-Fluoro anilinium nitrate | 7.37-7.42 (m 1H), 6.93–7.00 (m 3H), 5.34 (br s 3H, $NH_3^+$) | 7.42-7.47 (m 1H), 7.00-7.10 (m 3H) |
| 4-Chloro anilinium nitrate | 8.85 (br s 3H, $NH_3^+$), 7.50 (d 2H, *J* = 8.0), 7.25 (d 2H, *J* = 7.6) | 8.95 (br s 3H, $NH_3^+$), 7.53 (d 2H, *J* = 8.8), 7.30 (d 2H, *J* = 8.8) |
| 4-Bromo anilinium nitrate | 8.63 (br s 3H $NH_3^+$), 7.60 (d 2H, *J* = 7.2), 7.16 (d 2H, *J* = 6.8) | 8.80 (br s 3H, $NH_3^+$), 7.60 (d 2H, *J* = 9.2), 7.16 (d 2H, *J* = 9.2) |
| 4-Methyl anilinium nitrate | 9.83 (br s 3H, $NH_3^+$), 7.30 (d 2H, *J* = 8.0), 7.23 (d 2H, *J* = 8.0), 2.32 (s 3H) | 9.96 (br s 3H, $NH_3^+$), 7.30 (d 2H, *J* = 8.4), 7.25 (d 2H, *J* = 8.4), 2.32 (s 3H) |
| 3-Methyl anilinium nitrate | 9.65 (br s 3H $NH_3^+$), 7.36 (t 1H, *J* = 8.0), 7.20 (d 1H, *J* = 7.6), 7.10 (d 2H, *J* = 5.6), 2.34 (s 3H) | 9.71 (br s 3H $NH_3^+$), 7.37 (t 1H *J* = 8.0), 7.21 (d 1H *J* = 7.6), 7.11 (d 2H *J* = 5.6), 2.34 (s 3H) |
| 2-Methyl anilinium nitrate | 9.57 (br s 3H, $NH_3^+$), 7.27–7.34 (m 4H), 2.30 (s 3H) | 9.73 (br s 3H, $NH_3^+$), 7.30–7.36 (m 4H), 2.31 (s 3H) |
| Benzilinium nitrate | 8.19 (s 3H, $NH_3^+$), 7.37–7.47 (m 5H), 4.05 (s 2H) | 8.20 (s 3H, $NH_3^+$), 7.38–7.45 (m 5H), 4.05 (q 2H, *J* = 5.8) |

| | | |
|---|---|---|
| (*R*)-Methyl benzilinium nitrate | 8.18 (br s 3H, $NH_3^+$), 7.36–7.49 (m 5H), 4.42 (q 1H, *J* = 6.8), 1.48 (d 3H, *J* = 6.8) | 8.27 (s 3H, $NH_3^+$), 7.36–7.49 (m 5H), 4.42 (q 1H, *J* = 6.8), 1.48 (d 3H, *J* = 7.2) |
| (S)-Methyl benzilinium nitrate | 8.28 (br s 3H $NH_3^+$), 7.38–7.49 (m 5H), 4.44 (q 1H, *J* = 6.4), 1.49 (d 3H, *J* = 6.8) | 8.30 (s 3H $NH_3^+$), 7.36–7.49 (m 5H), 4.43 (q 1H, *J* = 6.4), 1.48 (d 3H *J* = 6.8) |
| Pyridinium nitrate | 8.82 (d 2H, *J* = 4.8), 8.33 (tt 1H, *J* = 7.2 and 8.3), 7.84 (t 2H, *J* = 7.0), 5.25 (br s 1H, $NH^+$) | 8.96 (dd 2H, $NH_2$, *J* = 6.6), 8.62 (tt 1H, *J* = 7.7 and 8.0), 8.90 (t 2H, *J* = 7.2), 5.78 (br s 1H, $NH^+$) |
| 4-Amino pyridinium nitrate | - | 13.14 (br s 1H, $NH^+$), 8.12 (d 2H), 8.05 (s 2H, $NH_2$), 6.78 (d 2H, *J* = 7.2) |
| 3-Amino pyridinium nitrate | 7.99 (m 2H), 7.60–7.64 (m 1H), 7.56 (d 1H, *J* = 8.8), 6.18 (vbr s 3H $NH_2$ and $NH^+$ merge) | 14.89 (br s 1H, $NH^+$), 8.84 (br s 2H, $NH_2$), 8.00–8.02 (m 2H), 7.61–7.69 (m 2H) |
| 2-Amino pyridinium nitrate | 13.32 (br s 1H, $NH^+$), 7.97 (br s 2H $NH_2$), 7.90–7.95 (m 2H), 6.97 (d 1H, *J* = 9.6), 6.86 (t 1H, *J* = 6.6 and 6.8) | 13.32 (br s 1H, $NH^+$), 7.97 (br s 2H $NH_2$), 7.90–7.95 (m 2H), 6.97 (d 1H, *J* = 9.6), 6.86 (t 1H, *J* = 6.6 and 6.8) |
| 4-Hydroxy pyridinium nitrate | 13.08 (br s 1H, $NH^+$), 8.56 (d 2H, *J* = 7.6), 7.24 (d 2H, *J* = 7.6), 5.77 (s 1H) | 13.65 (br s 1H, $NH^+$), 8.59 (d 2H, *J* = 7.6), 7.25 (d 2H, *J* = 7.6) |
| Phenyl hydrazinium nitrate | 9.76 (br s 3H, $NH_3^+$), 8.33 (s 1H, NH), 7.49 (tt 2H, *J* = 7.2 and 8.0), 7.39 (tt 1H, J = 7.5), 7.32 (dt 2H, *J* = 6.9) | - |

The growth of anilinium nitrate-I leaves behind hard cocoon shaped particles, the solid state $^{27}Al$ NMR study on cocoon shaped material showed signature for alumina [23]. The $^{27}Al$ NMR of alumina is shown in Figure 8.4.

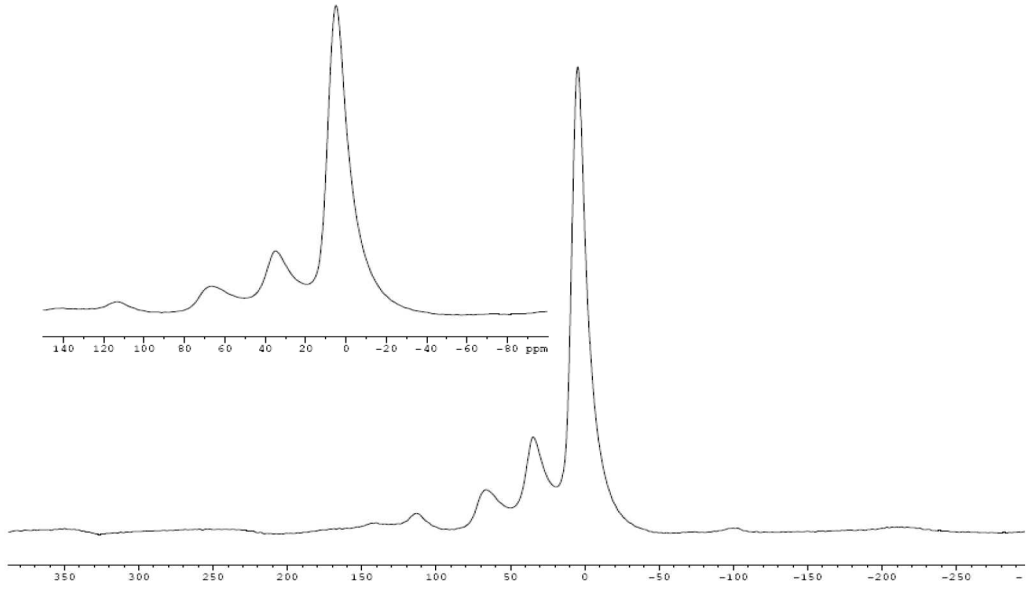


**Figure 8.4** $^{27}Al$ NMR spectra of rosette shaped alumina, recorded at MAS frequency of 10 kHz.

### 8.3.4 Thermal analyses

#### 8.3.4.1 Thermogravimetry/Differential Thermal Analysis (TG/DTA)

TG/DTA measurements on OANSs exothermic decomposition observed for almost all nitrate salts at different temperature except 3-fluoro anilinium nitrate-II and 4-bromo anilinium nitrate (I and II). The thermal analyses showed decomposition at 538 K for ammonium nitrate-II and around 490 K for anilinium nitrate (I and II). The details of TG/DTA are given in Table 8.4. The decomposition temperatures of substituted anilinium nitrate (I and II) are shifted at lower temperature as compared to anilinium nitrate (I and II) except 4-chloro anilinium nitrate (I and II), 4-fluoro anilinium nitrate-II, 3-methyl anilinium nitrate-II, and 4-methyl anilinium nitrate-II. On the other hand decomposition temperature of benzilinium nitrate, (*R*)- and (*S*)-methyl benzilinium nitrate, pyridinium nitrate and substituted pyridinium nitrate (I and II) are shifted to higher temperature as compared to anilinium nitrate. TG/DTA thermogram of some OANSs is showing almost complete weight loss (~95 %) followed by ignition (Figure 8.5), but in some cases showed incomplete weight loss (~80 %) see Figure 8.6. TG/DTA measurement shown OANSs salts have interesting decomposition pathways in which all nitrate salts are loses organic amine along with nitric acid, but 4-Chloro anilinium nitrate, 4-bromo anilinium nitrate (I and II), 3-amino pyridinium nitrate-II, and phenyl hydrazinium nitrate-I loses first nitric acid then organic amine Figure 8.7.

DTA analyses showed endothermic peak before the degradation, except 4-bromo anilinium nitrate, 2-methyl anilinium nitrate (I and II), phenyl hydrazinium nitrate-I, 4-hydroxy pyridinium nitrate-I and 3-amino pyridinium nitrate-II. The first endothermic peak of 3-methyl anilinium nitrate, benzilinium nitrate, 2-amino pyridinium nitrate (I and II), 3-amino pyridinium nitrate-I, and 4-amino pyridinium nitrate-II are characteristics for solid-liquid phase transitions. While for the other nitrate salts the first endothermic peaks are characteristics for solid-solid phase transition see Table 8.5.

We have checked the melting point of all the nitrate salts using capillary in paraffin oil. The melting temperatures of compounds correlate well with an endothermic peak of DTA, which characteristics for solid-liquid phase transitions.

**Table 8.4** TG/DTA of OANSs, showing thermal decomposition pathway

| Compounds | Organic ammonium nitrate-I | | | | | Organic ammonium nitrate-II | | | | |
|---|---|---|---|---|---|---|---|---|---|---|
| | Temperature [K] | TG [%] Theory | TG [%] Found | Possibility | DTA [uV] | Temperature [K] | TG [%] Theory | TG [%] Found | Possibility | DTA [uV] |
| Ammonium nitrate | No hair-like crystal observed | | | | | 538.1 | 100.00 | 99.69 | $NH_4^+NO_3^-$ | 45.7 |
| Anilinium nitrate | 488.2 | 100.00 | 93.00 | $C_6H_5NH_3^+NO_3^-$ | 93.9 | 491.4 | 100.00 | 95.89 | $C_6H_5NH_3^+NO_3^-$ | 47.3 |
| 4-Fluoro anilinium nitrate | 481.7 | 100.00 | 93.80 | $4\text{-}F\text{-}C_6H_4NH_3^+NO_3^-$ | 12.7 | 494.0 | 100.00 | 79.14 | $4\text{-}F\text{-}C_6H_4NH_3^+NO_3^-$ | 89.5 |
| 3-Fluoro anilinium nitrate | 471.2 | 100.00 | 93.13 | $3\text{-}F\text{-}C_6H_4NH_3^+NO_3^-$ | 13.3 | 450.1 | 100.00 | 95.78 | $3\text{-}F\text{-}C_6H_4NH_3^+NO_3^-$ | -6.7 |
| 4-Chloro | 453.4 | 33.06 | 16.19 | $HNO_3$ | -27.3 | 452.5 | 33.06 | 22.92 | $HNO_3$ | -13.4 |
| anilinium nitrate | 511.5 | 66.94 | 72.78 | $4\text{-}Cl\text{-}C_6H_4NH_2$ | 25.6 | 492.5 | 66.94 | 68.56 | $4\text{-}Cl\text{-}C_6H_4NH_2$ | 13.2 |
| 4-Bromo | 440.1 | 26.81 | 21.53 | $HNO_3$ | -7.2 | 436.8 | 26.81 | 22.87 | $HNO_3$ | -3.0 |
| anilinium nitrate | 471.7 | 73.19 | 73.27 | $4\text{-}Br\text{-}C_6H_4NH_2$ | -8.7 | 467.7 | 73.19 | 70.27 | $4\text{-}Br\text{-}C_6H_4NH_2$ | -2.0 |
| 4-Methyl anilinium nitrate | 470.9 | 100.00 | 86.77 | $4\text{-}CH_3\text{-}C_6H_4NH_3^+NO_3^-$ | 23.3 | 516.0 | 100.00 | 80.19 | $4\text{-}CH_3\text{-}C_6H_4NH_3^+NO_3^-$ | 178.1 |
| 3-Methyl anilinium nitrate | 478.8 | 100.00 | 94.12 | $3\text{-}CH_3\text{-}C_6H_4NH_3^+NO_3^-$ | 14.6 | 495.4 | 100.00 | 89.69 | $3\text{-}CH_3\text{-}C_6H_4NH_3^+NO_3^-$ | 56.1 |
| 2-Methyl anilinium nitrate | 480.6 | 100.00 | 92.46 | $2\text{-}CH_3\text{-}C_6H_4NH_3^+NO_3^-$ | 32.8 | 475.7 | 100.00 | 85.42 | $2\text{-}CH_3\text{-}C_6H_4NH_3^+NO_3^-$ | 40.6 |
| Benzilinium nitrate | 531.9 | 100.00 | 95.74 | $C_6H_5CH_2NH_3^+NO_3^-$ | 42.9 | 534.1 | 100.00 | 98.32 | $C_6H_5CH_2NH_3^+NO_3^-$ | 85.9 |

| | | | | | | | | | | |
|---|---|---|---|---|---|---|---|---|---|---|
| (*R*)-Methyl benzilinium nitrate | 525.1 | 100.00 | 95.19 | $C_6H_5CH(CH_3)NH_3^+NO_3^-$ | 145.1 | 505.9 | 100.00 | 93.40 | $C_6H_5CH(CH_3)NH_3^+NO_3^-$ | 34.9 |
| (S)-Methyl benzilinium nitrate | 512.8 | 100.00 | 77.99 | $C_6H_5CH(CH_3)NH_3^+NO_3^-$ | 53.9 | 529.8 | 100.00 | 95.08 | $C_6H_5CH(CH_3)NH_3^+NO_3^-$ | 182.2 |
| Pyridinium nitrate | 486.5 | 100.00 | 89.14 | $C_5H_5NH^+NO_3^-$ | -7.8 | 536.3 | 100.00 | 75.34 | $C_5H_5NH^+NO_3^-$ | 29.3 |
| 4-Amino pyridinium nitrate | No hair-like crystal observed | | | | | 547.2 | 100.00 | 96.97 | $4\text{-}NH_2\text{-}C_5H_4NH^+NO_3^-$ | 133.1 |
| 3-Amino pyridinium nitrate | 557.3 | 100.00 | 75.76 | $3\text{-}NH_2\text{-}C_5H_4NH^+NO_3^-$ | 129.3 | 400.5 | 40.10 | 25.22 | $HNO_3$ | -16.3 |
| | | | | | | 528.8 | 59.90 | 56.02 | $3\text{-}NH_2\text{-}C_5H_4N$ | 88.5 |
| 2-Amino pyridinium nitrate | 497.6 | 100.00 | 88.03 | $2\text{-}NH_2\text{-}C_5H_4NH^+NO_3^-$ | 113.6 | 504.3 | 100.00 | 89.08 | $2\text{-}NH_2\text{-}C_5H_4NH^+NO_3^-$ | 87.3 |
| 4-Hydroxy pyridinium nitrate | 503.1 | 100.00 | 79.58 | $4\text{-}OH\text{-}C_5H_4NH^+NO_3^-$ | 137.9 | No sugar-like crystal observed | | | | |
| Phenyl hydrazinium nitrate | 367.0 | 36.82 | 11.48 | $HNO_3$ | 8.24 | No sugar-like crystal observed | | | | |
| | 478.4 | 63.18 | 77.60 | $C_6H_5NHNH_2$ | 20.3 | | | | | |

While some nitrate salts do not melt up to the degradation temperature. All nitrates salts are highly fuel rich and a black residue remain in crucible after decomposition. The exothermic peak are characteristic for oxidation reduction reactions between oxidizer part ($NO_3^-$) and fuel part (organic ammonium cations) leading to ignition to produce gaseous products along with a residual carbon [24]. The overall decomposition of these salts initiate by transfer of a proton from ammonium ions ($R\text{-}NH_3^+$) to nitrate anions ($NO_3^-$) molecule in condensed phase before ignition [24]. Experimental thermal analyses indicates methyl ammonium nitrate dissociates to form methyl amine and nitric acid at 573 K, which on further heating decomposes to form varied compounds including nitrogen oxides and nitrous acid with liberation of heat [25].

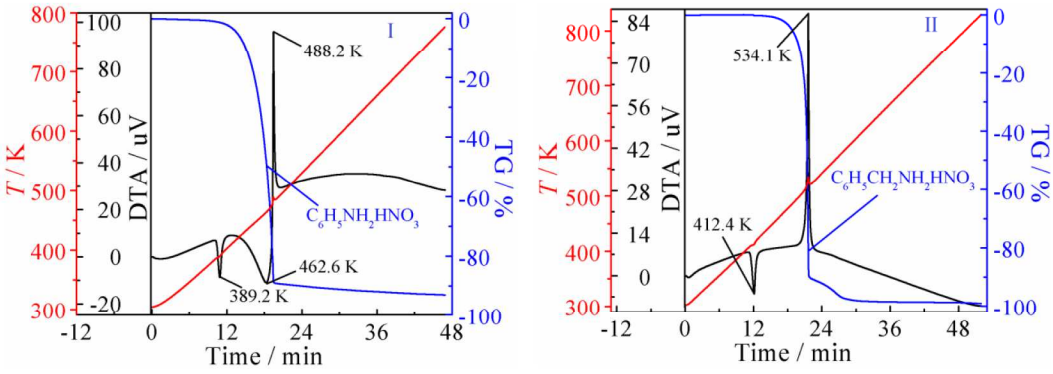


(a) (b)

**Figure 8.5** TG/DTA thermograms of anilinium nitrate-I (a) and benzilinium nitrate-II (b).

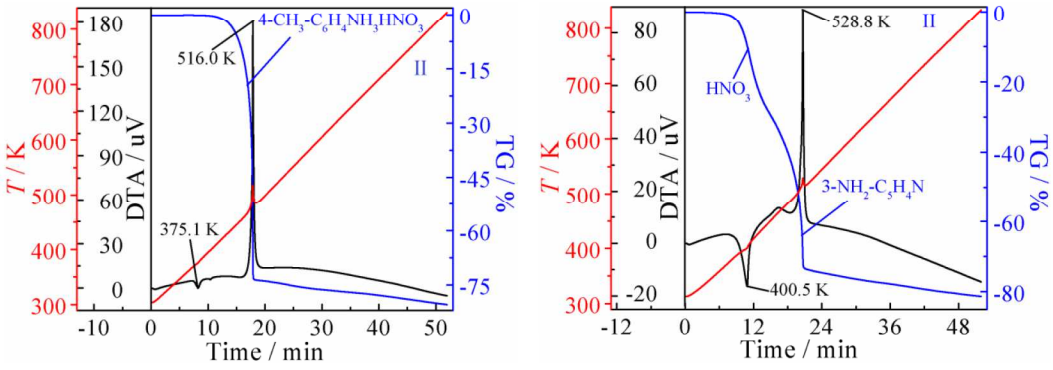


(a) (b)

**Figure 8.6** TG/DTA thermograms of 4-methyl anilinium nitrate-II (a) and 3-amino pyridinium nitrate-II (b).

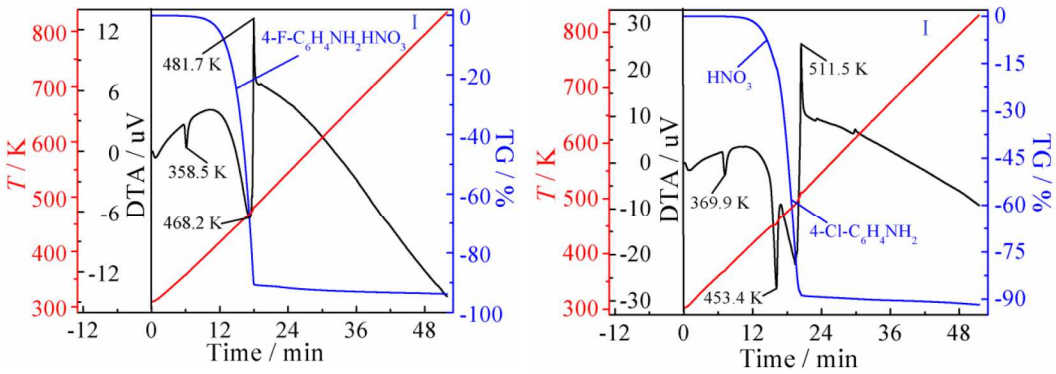


(a) (b)

**Figure 8.7** TG/DTA thermograms of 4-fluoro anilinium nitrate-I (a) and 4-chloro anilinium nitrate-I (b).

### 8.3.4.2 Differential Scanning Calorimetry (DSC)

DSC measurements for all OANSs were performed before an onset of mass loss starts as observed in TG/DTA analysis. DSC measurements on anilinium nitrate (I and II) showed one endothermic peak at 390.03 K (-40.16 $Jg^{-1}$) and 381.38 K (-45.57 $Jg^{-1}$) while heating and one exothermic peak at 337.79 K (49.56 $Jg^{-1}$) and 364.59 K (47.74 $Jg^{-1}$) while cooling, characteristic for solid-solid phase transition see Figure 8.8 (a). For the conformation this solid-solid phase transition in anilinium nitrate-I, we have repeated DSC measurements for number of heating and cooling cycles on the same samples. We observed not only endothermic and exothermic transition temperature similar but their enthalpies is also same, see Figure 8.8 (b). Compounds 3-fluoro anilinium nitrate, 4-fluoro anilinium nitrate, 4-chloro anilinium nitrate and benzilinium nitrate also showed one endothermic peak while heating and one exothermic peak while cooling similarly to anilinium nitrate, characteristic for solid-solid phase transition. Interestingly DSC studied on (*R*)- and (*S*)-methyl benzilinium nitrate salts; (*R*)-methyl benzilinium nitrate-I showed two endothermic peaks while heating and one exothermic peak while cooling, while (*S*)-methyl benzilinium nitrate-I are showing two endothermic peaks while heating and two endothermic peaks while cooling. In case of (*R*)-methyl benzilinium nitrate-I two endothermic peaks observed at 365.82 K (-2.54 J $g^{-1}$) and 373.02 K (-4.55 J $g^{-1}$) while heating in which first peak characteristic for solid-solid phase transition and second peak characteristic for solid-liquid phase transitions, and one exothermic peak observed at 314.62 K (41.90 J $g^{-1}$)

while cooling, characteristic for liquid-solid phase transitions see Figure 8.9 (a). For compound (*S*)-methyl benzilinium nitrate-I peak observed at 362.74 K (-10.13 J $g^{-1}$) while heating, and at 308.78 K (4.27 J $g^{-1}$) while cooling, characteristic for solid-solid phase transition and peak observed at 377.77 K (-49.50 J $g^{-1}$) while heating, characteristic for solid-liquid phase transition and peak observed at 314.23 K (42.14 J $g^{-1}$) while cooling is characteristic for liquid-solid phase transition as shown in Figure 8.9 (b).

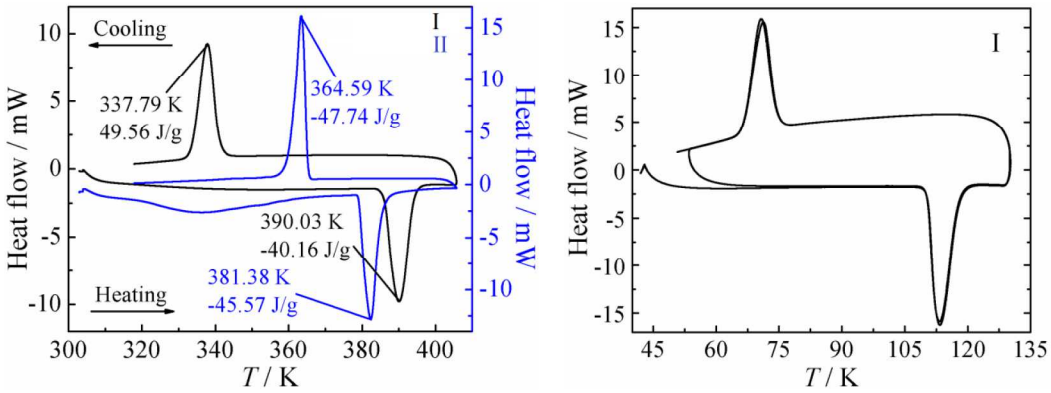


**Figure 8.8** DSC Thermogram of anilinium nitrate (I and II) (a) and anilinium nitrate-I repeated heating and cooling cycle (b).

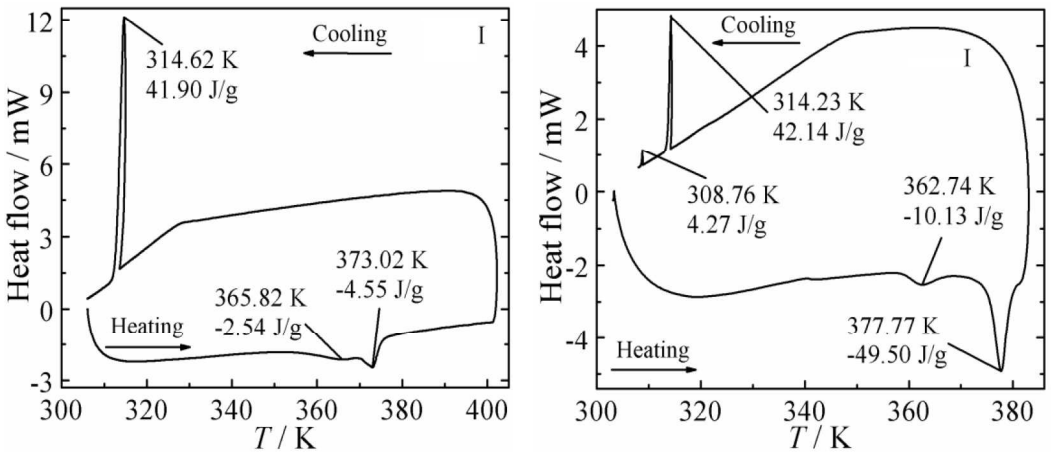


**Figure 8.9** DSC Thermogram of (*R*)- and (*S*)-methyl benzilinium nitrate-I (a) and (b).

**Table 8.5** DSC transition of OANSs

| Compounds | Organic ammonium nitrate-I | | | | Organic ammonium nitrate-II | | | |
|---|---|---|---|---|---|---|---|---|
| | Heating | | Cooling | | Heating | | Cooling | |
| | Transition temperature [K] | Enthalpy [J $g^{-1}$] | Transition temperature [K] | Enthalpy [J $g^{-1}$] | Transition temperature [K] | Enthalpy [J $g^{-1}$] | Transition temperature [K] | Enthalpy [J $g^{-1}$] |
| Ammonium nitrate | No hair crystal observed | | | | 256.31 | -11.26 | 234.60 | 2.12 |
| | | | | | 267.12 | -0.83 | 238.91 | 5.40 |
| | | | | | 326.28 | -11.86 | 318.56 | 20.90 |
| | | | | | 362.01 | -10.80 | | |
| | | | | | 400.74 | -34.86 | 391.11 | 31.40 |
| Anilinium nitrate | 390.03 | -40.16 | 337.79 | 49.56 | 381.38 | -45.57 | 364.59 | 47.74 |
| 4-Fluoro anilinium nitrate | 359.24 | -17.70 | 352.46 | 17.41 | 356.77 | -18.24 | 350.45 | 19.14 |
| 3-Fluoro anilinium nitrate | 381.90 | -14.97 | 375.01 | 16.44 | 383.03 | -14.31 | 376.68 | 17.61 |
| 4-Chloro anilinium nitrate | 366.77 | -5.79 | 360.10 | 6.28 | 366.70 | -18.04 | 360.51 | 18.94 |
| 4-Bromo anilinium nitrate | No transition observed | | | | No transition observed | | | |
| 4-Methyl anilinium nitrate | 353.97 | -14.22 | | | 355.05 | -30.71 | | |
| | 371.95 | -11.76 | | | 372.59 | -3.95 | | |
| | 396.65 | -6.43 | 392.84 | 5.53 | 396.94 | -5.32 | 392.34 | 5.30 |
| 3-Methyl anilinium nitrate | No transition observed | | | | No transition observed | | | |
| 2-Methyl anilinium nitrate | No transition observed | | | | No transition observed | | | |
| Benzilinium nitrate | 225.90 | -5.14 | 203.86 | 4.86 | No transition observed | | | |
| (*R*)-Methyl benzilinium nitrate | 365.82 | -2.54 | No transition observed | | No transition observed | | | |
| (S)-Methyl benzilinium nitrate | 362.74 | -10.13 | 308.76 | 4.27 | No transition observed | | | |
| Pyridinium nitrate | No transition observed | | | | No transition observed | | | |
| 4-Amino pyridinium nitrate | No transition observed | | | | No transition observed | | | |
| 3-Amino pyridinium nitrate | No transition observed | | | | No transition observed | | | |
| 2-Amino pyridinium nitrate | No transition observed | | | | No transition observed | | | |
| 4-Hydroxy pyridinium nitrate | No transition observed | | | | No transition observed | | | |
| Phenyl hydrazinium nitrate | No transition observed | | | | | | | |

Furthermore, DSC studies on 4-bromo anilinium nitrate, 2-methyl anilinium nitrate, 3-methyl anilinium nitrate, pyridinium nitrate, amino substituted pyridinium nitrate, 4-hydroxy pyridinium nitrate (I and II) and phenyl hydrazinium nitrate-I did not represent any information of solid-solid phase transition. The details of measured transition temperatures and enthalpies for OANSs are given in Table 8.5.

Benzilinium nitrate-II shows phase change at 227.0 K (-5.29 J $g^{-1}$) [26], is reported in literature, so we did DSC measurement at LT twice for benzilinium nitrate (I and II), we did not get any information up to this temperature range for benzilinium nitrate-II and we get the one endothermic peak at 225.90 K (-5.14 $Jg^{-1}$) while heating and one exothermic peak at 203.86 K (4.86 $Jg^{-1}$) while cooling for benzilinium nitrate-I, characteristic for solid-solid phase change see Figure 8.10 (a). We have also collected the single crystal data at 150 K and 296 K for benzilinium nitrate-II, but did not observe any structural change. The three characteristic peaks for 4-methyl anilinium nitrate (I and II) were determined in temperature range 351.4 K - 399.4 K Figure 8.10 (b).

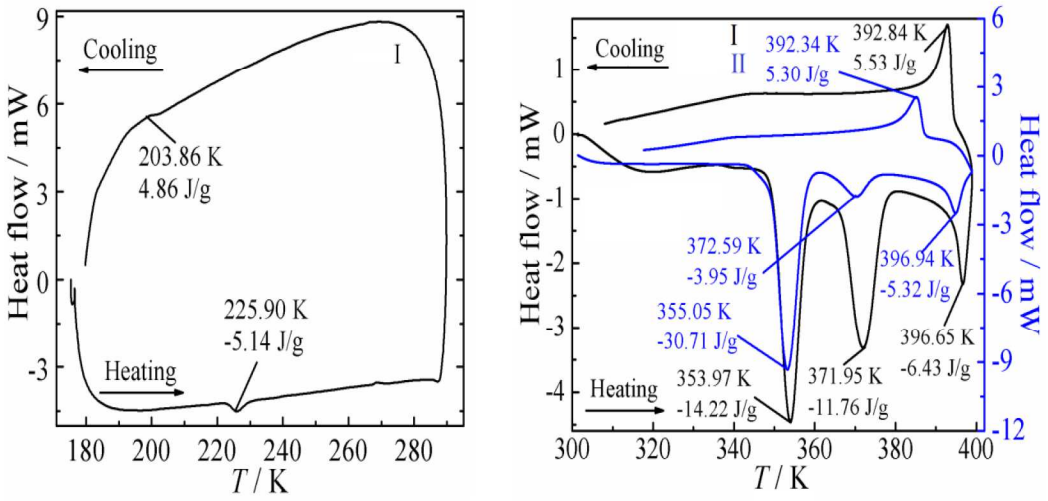


(a) (b)

**Figure 8.10** DSC Thermogram of benzilinium nitrate-I (a) and 4-methyl anilinium nitrate (I and II) (b).

Single crystal XRD study on 4-methyl anilinium nitrate-II showed it has monoclinic space group $P2_1/n$ at 100 K [27] which changes to space group $P2_1/c$ at RT [28]. To confirm this transition we carried out LT DSC (153 K - 308 K) on 4-methyl anilinium nitrate (I and II), but we could not observe any transition at LT, but

we get three endothermic peaks while heating and one exothermic peak while cooling at HT. If we consider 4-methyl anilinium nitrate exists in $\alpha$ phase at lower temperatures, then according to DSC studies the second phase transitions is $\beta \rightarrow \gamma$, should be between 153 K and 355.1 K. The next phase transformation, $\gamma \rightarrow \delta$ and $\delta \rightarrow \varepsilon$ are around 372.6 K (-3.95 J $g^{-1}$) and 396.9 K (-5.32 J $g^{-1}$). During cooling, only one exothermic peak was observed at 392.3 K (5.30 J $g^{-1}$), may be characteristic for $\varepsilon \rightarrow \delta$ *or* or $\varepsilon \rightarrow \gamma$. We observed similar peak patterns for 4-methyl ammonium nitrate, when re-recorded after one hour. This was very similar to the behavior of ammonium nitrate-II, as shown in Figure 8.11 [1,29].

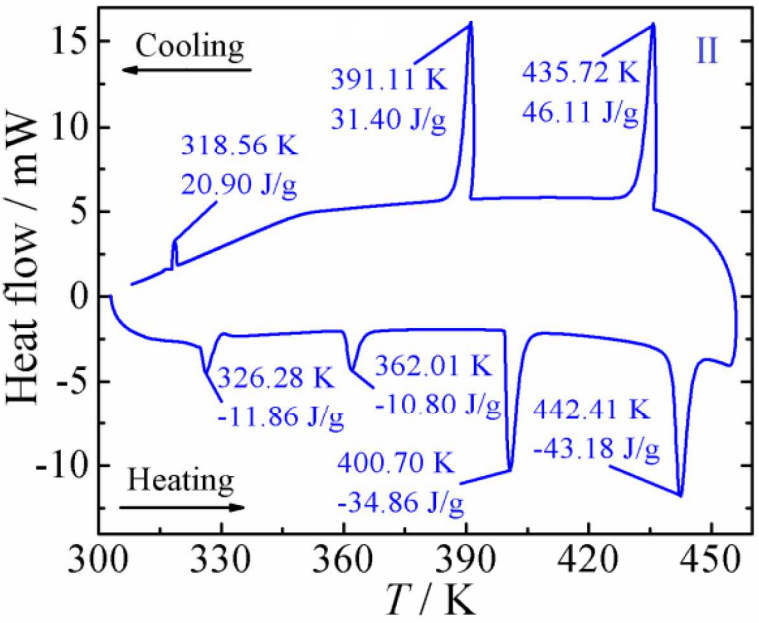


(a)

**Figure 8.11** DSC Thermogram of ammonium nitrate-II at HT.

## 8.3.5 Crystal structure

### 8.3.5.1 Single Crystal X-ray Diffraction

The details of the crystallographic data collection parameters and refinement data for anilinium nitrate-II, 4-methyl anilinium nitrate-II and benzilinium nitrate-II are given in Table 8.6. Figure 8.12 shows the asymmetric unit consists of a anilinium nitrate-II, 4-methyl anilinium nitrate-II and benzilinium nitrate-II.

**Table 8.6** Crystallographic data and structure refinements for anilinium nitrate-II, 4-methyl anilinium nitrate-II and benzilinium nitrate-II salts

| **Compounds** | **Anilinium nitrate-II** | **4-Methyl anilinium nitrate-II** | **Benzilinium nitrate-II** |
|---|---|---|---|
| Formula | $C_6H_8N_2O_3$ | $C_7H_{10}N_2O_3$ | $C_7H_{10}N_2O_3$ |
| Formula weight | 156.14 | 170.17 | 170.17 |
| Temperature [K] | 293 | 150 | 296 |
| Wave length [Å] | 0.71073 | 0.71073 | 0.71073 |
| Crystal system | Orthorhombic | Monoclinic | Orthorhombic |
| Space group | *Pbca* | $P2_1/n$ | *Pbca* |
| *a* [Å] | 10.158(2) | 5.6677(5) | 10.6597(3) |
| *b* [Å] | 9.277(2) | 8.5764(8) | 10.1594(2) |
| *c* [Å] | 16.177(3) | 17.6199(14) | 16.4923(4) |
| $\beta$ (°) | 90 | 99.026(5) | 90 |
| *V* [Å$^3$] | 1524.5(5) | 845.87(13) | 1786.05(8) |
| *Z* | 8 | 4 | 8 |
| $D_{calc}$ [mg/m$^3$] | 1.361 | 1.336 | 1.266 |
| Crystal size [mm$^3$] | 0.32×0.26×0.14 | 0.24×0.04×0.04 | 0.42×0.24×0.20 |
| *F*(000) | 656 | 360 | 720 |
| 2$\theta$ range [°] | 2.98 – 29.53 | 2.34 - 27.09 | 2.47 - 26.36 |
| Index ranges | -13 ≤ h ≤ 13,<br>-12 ≤ k ≤ 10,<br>-21 ≤ l ≤ 21 | -7 ≤ h ≤ 6,<br>-5 ≤ k ≤ 10,<br>-22 ≤ l ≤ 21 | -13 ≤ h ≤ 9,<br>-11 ≤ k ≤ 12,<br>-13 ≤ l ≤ 20 |
| Reflection collected | 13258 | 3814 | 7388 |
| Independent reflections | 2025 [$R_{(int)}$ = 0.0295] | 1852 [$R_{(int)}$ = 0.0445] | 1822 [$R_{(int)}$ = 0.0275] |
| Completeness to $\theta$ = 26.36° | 83.6 % | 99.5 % | 99.3 % |
| Goodness-of-fit on $F^2$ | 0.729 | 0.958 | 1.024 |
| Data / restraints / parameters | 2025 / 0 / 133 | 1852 / 0 / 149 | 1822 / 0 / 149 |
| Final *R* indices [$I>2\sigma(I)$] | *R1* = 0.0379,<br>w*R2* = 0.0854 | *R1* = 0.0497,<br>w*R2* = 0.1093 | *R1* = 0.0425,<br>w*R2* = 0.1191 |
| *R* indices (all data) | *R1* = 0.0758,<br>w*R2* = 0.1107 | *R1* = 0.1006,<br>w*R2* = 0.1345 | *R1* = 0.0668,<br>w*R2* = 0.1394 |

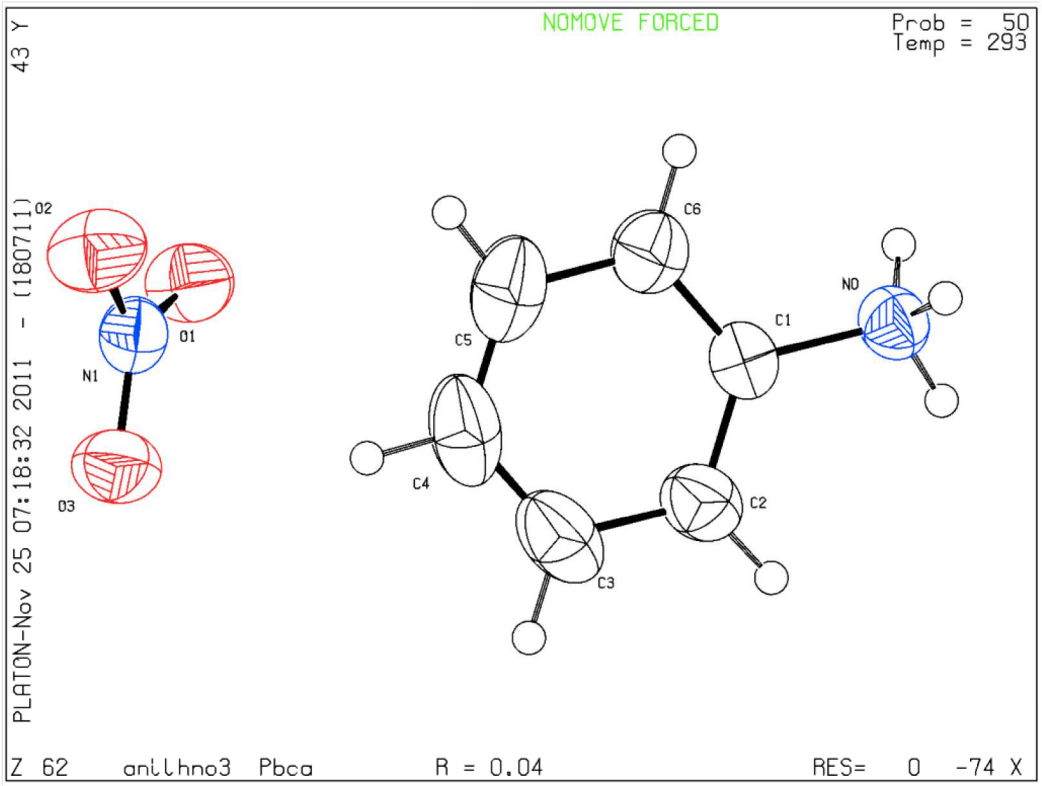
NOMOVE FORCED
Prob = 50
Temp = 293
43 Y
PLATON-Nov 25 07:18:32 2011 - (180711)
O2
O1
N1
O3
C6
N0
C1
C5
C4
C2
C3
Z 62 anilhno3 Pbca R = 0.04 RES= 0 -74 X

(a)

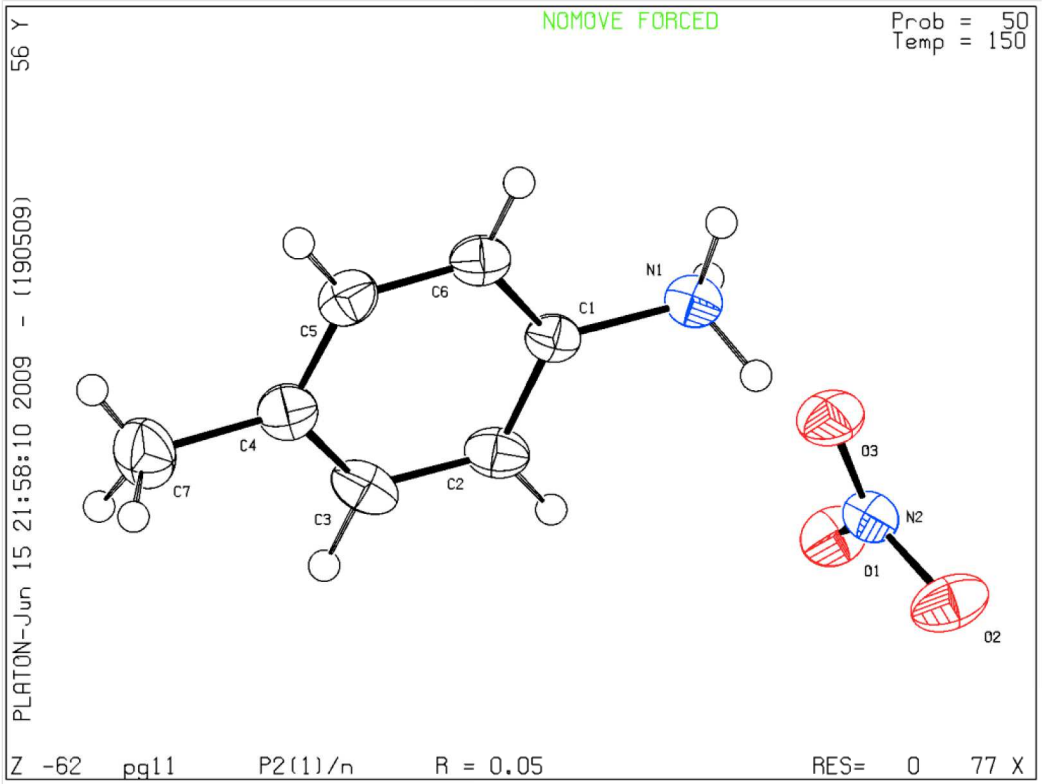
NOMOVE FORCED
Prob = 50
Temp = 150
56 Y
PLATON-Jun 15 21:58:10 2009 - (190509)
N1
C6
C1
C5
C4
C7
C2
C3
O3
N2
O1
O2
Z -62 pg11 P2(1)/n R = 0.05 RES= 0 77 X

(b)

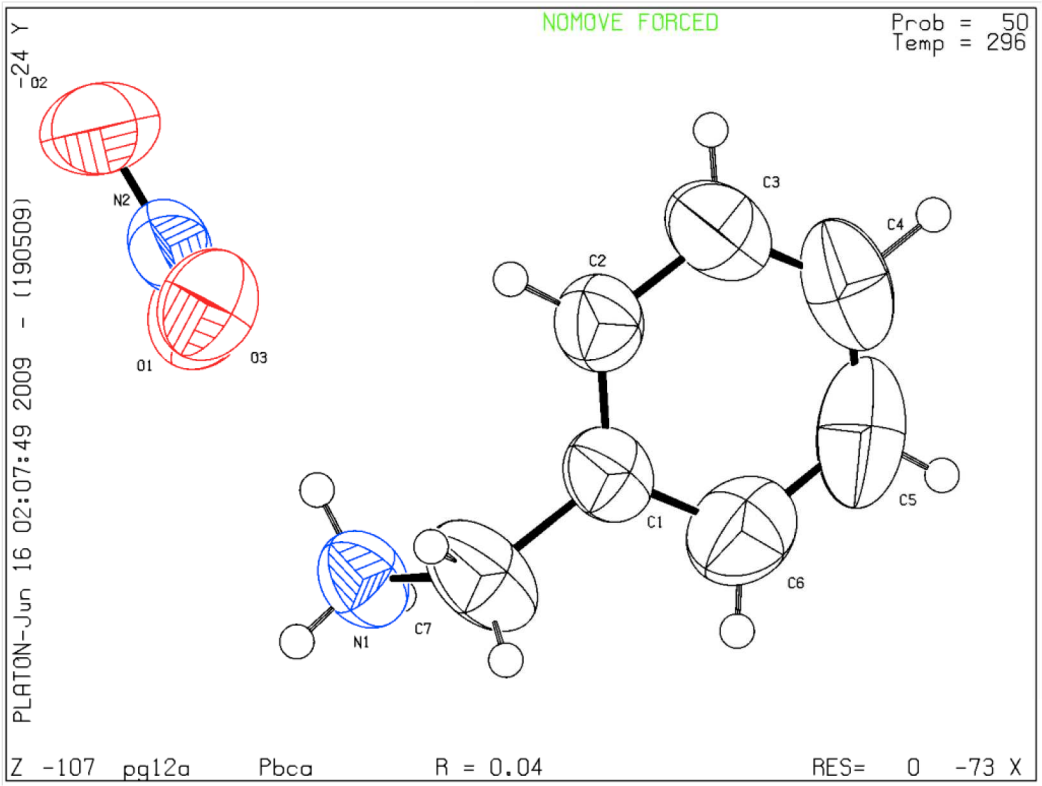


(c)

**Figure 8.12** Molecular views of Anilinium nitrate-II at 293 K (a); 4-methyl anilinium nitrate-II at 150 K (b) and benzilinium nitrate-II at 298 K (c), with labeling scheme, displacement ellipsoids are drawn at the 50 % probability level.

Single crystal XRD studies on anilinium nitrate-II, benzilinium nitrate-II and 4-methyl anilinium nitrate-II revealed that anilinium nitrate-II, benzilinium nitrate-II crystallized in orthorhombic space group, *Pbca* with unit cell dimensions $a$ = 10.158(2) Å, $b$ = 9.277(2) Å, $c$ = 16.177(3) Å, $V$ = 1524.5(5) Å$^3$ , $Z$ = 8 and $a$ = 10.659(2) Å, $b$ = 10.159(2) Å, $c$ = 16.493(2) Å, $V$ = 1786.1(2) Å$^3$, $Z$ = 8 respectively, while 4-methyl anilinium nitrate-II [25] crystallized in monoclinic space group $P2_1/c$ with cell dimensions $a$ = 5.647(2) Å, $b$ = 8.786(3) Å, $c$ = 17.811(4) Å, $V$ = 872.8(3) Å$^3$, $Z$ = 4. The primitive unit cell of anilinium nitrate-II, benzilinium nitrate-II contains eight molecules and 4-methyl anilinium nitrate-II contains four molecules. Monoprotonated benzilinium cation interacts through weak hydrogen bonds with three neighboring nitrates anions. The alternatively stacked benzilinium cations are hold together by oxygen of the nitrate anions and form penetrating chains. Anilinium nitrate-II and benzilinium nitrate-II although belong to same crystal system, but they

have different N-H···O pattern. In benzilinium nitrate-II specifically, two oxygen O(1) and O(3) of nitrate anions bond distance 1.242(2) Å and 1.240(2) Å bridges by two neighboring cations with N-H···O hydrogen bonds (bifurcated) distance 2.965(3) Å, 2.971(2) Å and 2.924(2) Å, 3.059(2) Å respectively, while third oxygen not involved in hydrogen bond. The N-O distances of benzilinium nitrate-II associated with doubly hydrogen bonded O(1) and O(3) is longest while non hydrogen bonded O(2) is shortest. The ammonium group of benzilinium nitrate-II accepts the two bifurcated N-H···O [angle 143.3(2)° - 163.7(2)° and 137.6(2)° - 165.7(2)°] interaction with different N···O and H···O bond distances as shown in Table 8.7. Thus one of the ammonium cation formed four N-H···O hydrogen bonds with four oxygen atoms of nitrates anion. In anilinium nitrate-II one oxygen atom O(1) bridged with two neighboring cations, O(2) bridged with one neighboring cation and O(3) not involved in hydrogen bond. The 4-methyl anilinium nitrate-II also shows one oxygen atom O(2) bridges with two neighboring cations, O(1) bridges with one neighboring cation and O(3) not involved in hydrogen bond. Although anilinium nitrate-II and 4-methyl anilinium nitrate-II formed three N-H···O hydrogen bonds with three oxygen atoms of nitrates anion with bifurcated N-H···O [angle 171.4(9)° - 177.2(9)° and 158.0(1)° - 168.7(1)° respectively] interaction, at different N···O and H···O bond distances (Table 8.7), but they have different N-H···O arrangement. View of crystal packing and hydrogen bonds for anilinium nitrate-II, benzilinium nitrate-II and 4-methyl anilinium nitrate-II are represented in Figure 8.13.

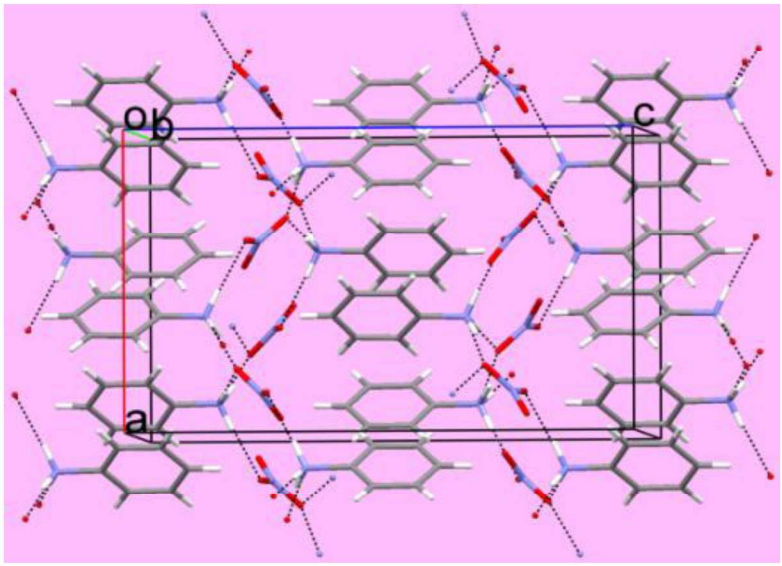


(a)

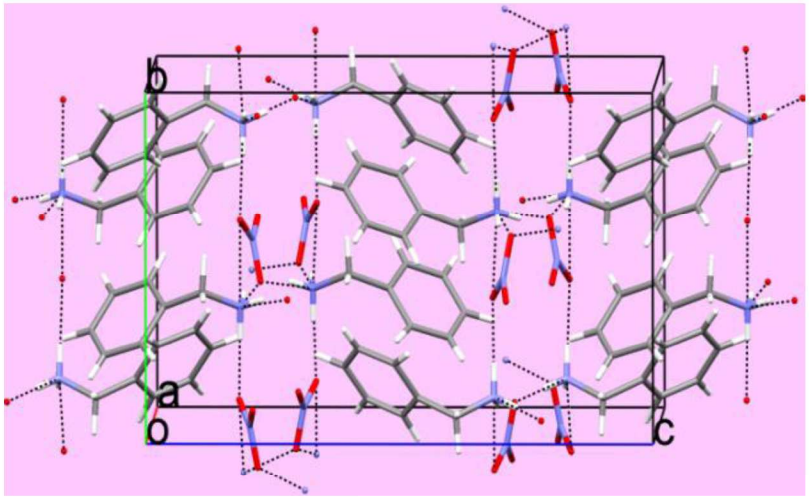


(b)

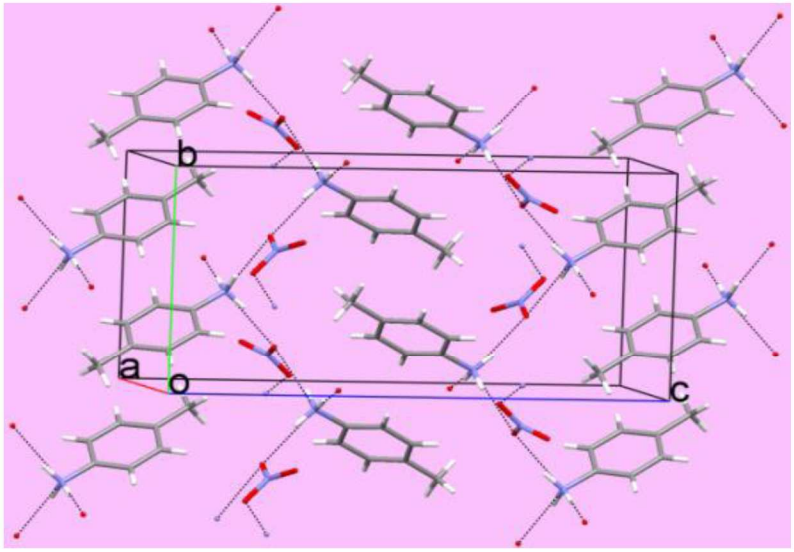


(c)

**Figure 8.13** A view of crystal packing of anilinium nitrate-II (a); benzilinium nitrate-II (b) and 4-methyl anilinium nitrate-II (c), N-H···O hydrogen bonds are shown as dashed lines.

In summary, benzilinium nitrate-II has been stabilized by four types of N-H···O interaction, while anilinium nitrate-II and 4-methyl anilinium nitrate-II have been stabilized by three types of N-H···O interaction. There are significant differences in N-H···O interaction present in the structure. In literature for anilinium nitrate, benzilinium nitrate and 4-methyl anilinium nitrate; anilinium nitrate-II at 293 K, benzilinium nitrate-II at 120 K [30] crystallized in orthorhombic space group *Pbca* and 4-methyl anilinium nitrate-II crystallized in monoclinic space group $P2_1/n$ at 100

K [27]. The distance between phenyl ring of neighboring cations in anilinium nitrate-II, benzilinium nitrate-II and 4-methyl anilinium nitrate-II are 3.808(1) Å, 3.884(4) Å and 3.777(3) Å respectively.

On the other hand, if we compared these crystals with ammonium nitrate. The ammonium nitrate have also significant different in N-H···O interaction at different temperature. These are well known to exist in five phases I, II, III, IV and V from 0 K to 442 K (melting point) [1]. The interaction of N-H···O chain between cation of R-$NH_3^+$ and anion of $NO_3^-$ in anilinium nitrate-II, benzilinium nitrate-II, 4-methyl anilinium nitrate-II, ammonium nitrate and methyl ammonium nitrate at different phase are shown in Figure 8.14. To summarize the N-H···O interaction, are shorter than sum of the van der Waals radii of H and O (2.7 Å) in all structures [31]. The persistence of N-H···O interaction in variety of crystal structures means that, it has structure directing even though it is a weak interaction. The hydrogen bond lengths and angles for anilinium nitrate-II, benzilinium nitrate-II, 4-methyl anilinium nitrate-II, ammonium nitrate and methyl ammonium nitrate at different phase are listed in Table 8.7.

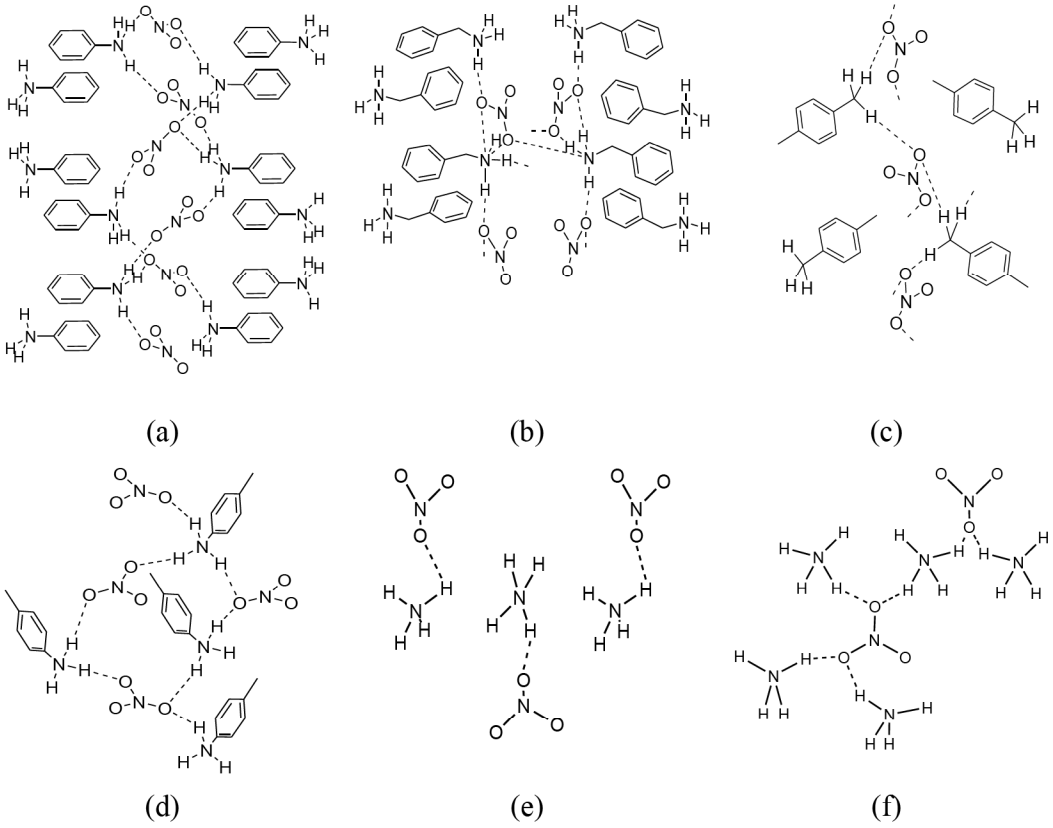

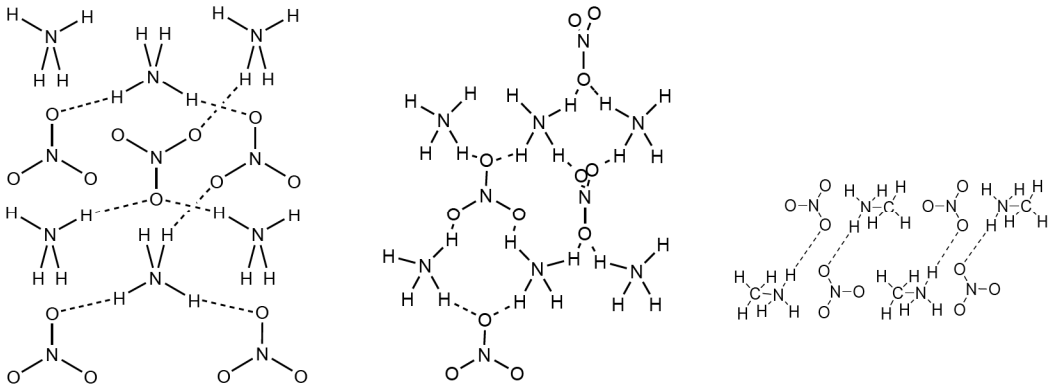

(g) (h) (i)

**Figure 8.14** N-H···O interactions in the crystal structure of anilinium nitrate-II at 293 K (a); benzilinium nitrate-II at 296 K (b); 4-methyl anilinium nitrate-II at 296 K (c), at 100 K (d); ammonium nitrate phase II at 357 K (e) [32], phase III at 318 K (f) [33], phase IV at 300 K (g) [34], phase V at 233 K (h) [35] and methyl ammonium nitrate at 300 K (i) [18].

**Table 8.7** Hydrogen bonds distances and angles [Å and °] for anilinium nitrate-II, benzilinium nitrate-II, 4-methyl anilinium nitrate-II, ammonium nitrate and methyl ammonium nitrate at different phase

| | **Distance** | | **Angle** |
|---|---|---|---|
| **Type of hydrogen bonds** | **N···O [Å]** | **H···O [Å]** | **N-H···O [°]** |
| | Anilinium nitrate-II at 293 K | | |
| N-H(1B)···O(1) | 2.860(1) | 1.923(9) | 177.2(9) |
| N-H(1C)···O(1) | 2.812(1) | 1.874(9) | 171.4(9) |
| N-H(1A)···O(2) | 2.879(1) | 1.970(9) | 175.6(8) |
| | Benzilinium nitrate-II at 296 K | | |
| N-H(1C)···O(1) | 2.971(2) | 2.259(3) | 143.3(2) |
| N-H(1A)···O(1) | 2.965(3) | 2.084(3) | 163.7(2) |
| N-H(1A)···O(3) | 3.059(2) | 2.328(3) | 137.6(2) |
| N-H(1B)···O(3) | 2.924(2) | 2.043(3) | 165.7(2) |
| | 4-Methyl anilinium nitrate-II at 296 K | | |
| N-H(1B)···O(1) | 2.847(2) | 1.965(2) | 171.1(1) |
| N-H(1C)···O(2) | 2.825(2) | 1.947(2) | 168.7(1) |
| N-H(1A)···O(2) | 2.974(2) | 2.131(2) | 158.0(1) |

| | | | |
|---|---|---|---|
| 4-Methyl anilinium nitrate-II at 100 K | | | |
| N-H(1A)···O(2) | 2.821(2) | 1.932(1) | 176.6(1) |
| N-H(1B)···O(3) | 2.803(2) | 1.929(1) | 167.2(1) |
| N-H(1C)···O(3) | 2.946(2) | 2.105(1) | 157.2(2) |
| Ammonium nitrate (II) at 357 K | | | |
| N-H(1A)···O(1) | 3.069(2) | 2.658(4) | 105.2(2) |
| N-H(1A)···O(2) | 2.981(4) | 2.008(6) | 163.3(4) |
| Ammonium nitrate (III) at 318 K | | | |
| N-H(1B)···O(1) | 3.032(5) | 2.330(7) | 138.5(4) |
| N-H(1C)···O(1) | 3.007(1) | 2.299(4) | 139.1(3) |
| N-H(1A)···O(2) | 3.132(4) | 2.395(4) | 147.0(2) |
| N-H(1C)···O(2) | 3.031(4) | 2.236(5) | 152.5(3) |
| Ammonium nitrate (IV) at 300 K | | | |
| N-H(1A)···O(1) | 2.971(3) | 2.050(7) | 154.4(8) |
| N-H(1B)···O(1) | 3.147(3) | 2.161(7) | 172.6(9) |
| N-H(1A)···O(2) | 3.200(4) | 2.326(7) | 147.0(9) |
| Ammonium nitrate (V) at 233 K | | | |
| N-H(1C)···O(1) | 2.932(6) | 1.958(8) | 147.4(3) |
| N-H(1D)···O(1) | 2.921(6) | 1.916(10) | 167.1(2) |
| N-H(1B)···O(2) | 2.931(8) | 1.939(11) | 164.7(2) |
| N-H(1A)···O(2) | 2.978(6) | 1.987(10) | 170.7(3) |
| Methyl ammonium nitrate at 300 K | | | |
| N-H(1B)···O(1) | 2.915(5) | 2.190(20) | 160.9(2) |
| N-H(1A)···O(2) | 2.885(3) | 2.190(20) | 156.4(2) |

CCDC No. 817532 and 817533 contains the crystallographic data for the compounds 4-methyl anilinium nitrate-II and benzilinium nitrate-II. This data can be obtained free of charge via http://www.ccdc.cam.ac.uk/conts/retrieving.html, or from the Cambridge Crystallographic Data Centre, 12 Union Road, Cambridge CB2 1EZ, UK; fax: (+44) 1223 336 033; or e-mail: deposit@ccdc.cam.ac.uk.

### 8.3.5.2 Powder X-ray Diffraction

Figure 8.15 show powder XRD pattern for anilinium nitrate-I, anilinium nitrate-II and anilinium nitrate-III. These powder patterns were indexed using powder X5

software, which verifies that, differs from each other, indicating 'polymorphism'. These powder patterns were indexed in orthorhombic lattice type *P* with unit cell dimensions $a$ = 10.148(2) Å, $b$ = 9.139(3) Å, $c$ = 16.177(3) Å, $V$ = 1504.68(9) Å$^3$, $R$ factor = 0.00247 for anilinium nitrate-I, $a$ = 10.131(5) Å, $b$ = 9.114(4) Å, $c$ = 16.147(2) Å, $V$ = 1496.88(10) Å$^3$, $R$ factor = 0.00208 for anilinium nitrate-II, and $a$ = 10.158(4) Å, $b$ = 9.277(4) Å, $c$ = 16.177(3) Å, $V$ = 1537.36 Å$^3$, $R$ factor = 0.00164 for anilinium nitrate-III. We have also collected the powder XRD data for anilinium nitrate-I at 298 K after reheated at 383 K. These indexed powder patterns were almost similar with anilinium nitrate-I but differ from anilinium nitrate-II as shown in Figure 8.16.

The hard cocoon shaped particles are left behind hair-like crystal growth of anilinium nitrate, look like hard materials. These cocoons were washed with methanol and dried at 343 K to obtain white crystalline powder. The powder XRD patterns of this white powder compound showed the signature of alumina see Figure 8.17.

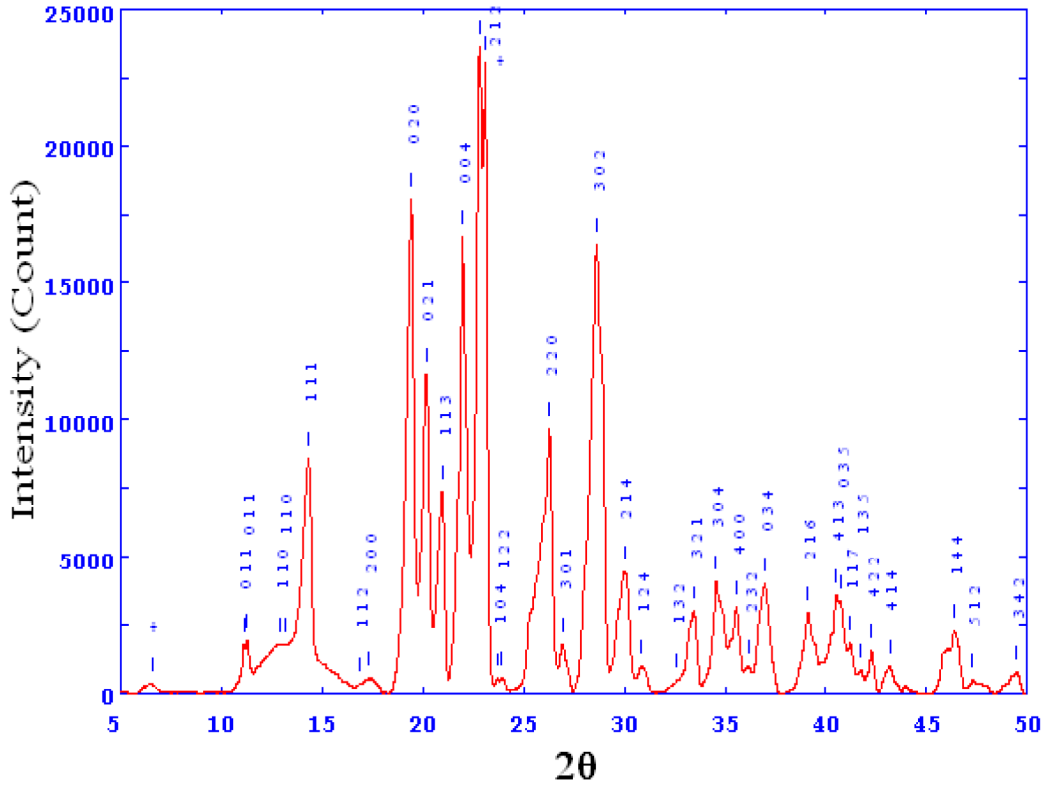


(a)

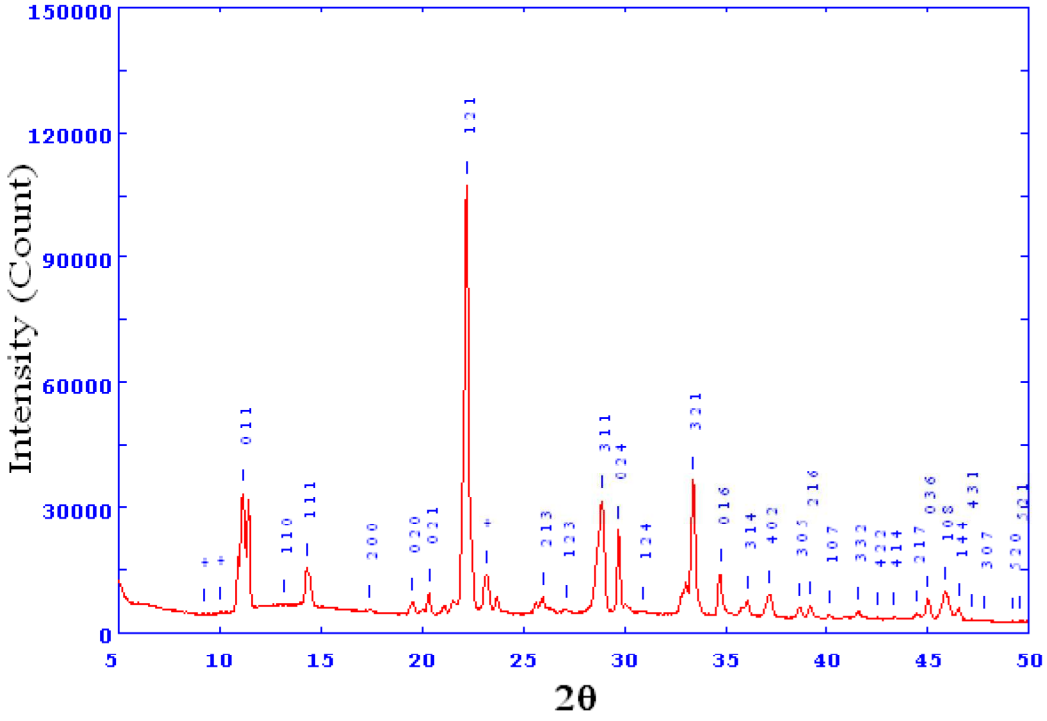


(b)

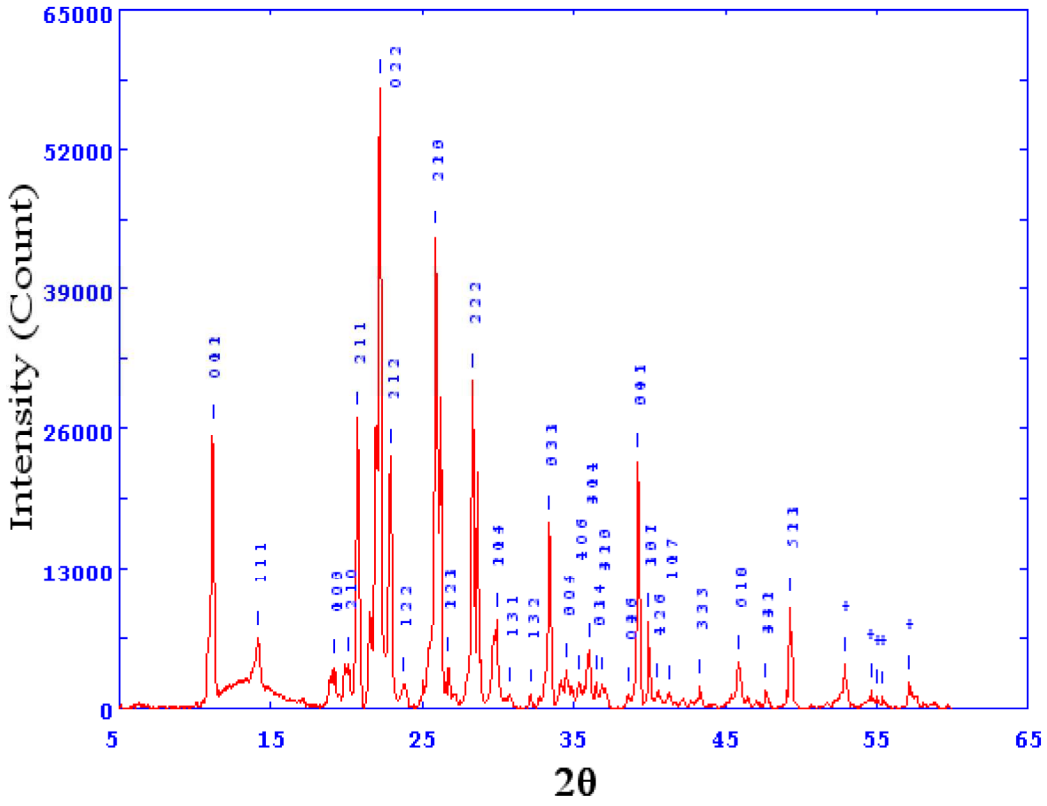


(c)

**Figure 8.15** Powder XRD data for Anilinium nitrate-I (a); Anilinium nitrate-II (b) and Anilinium nitrate-III (c).

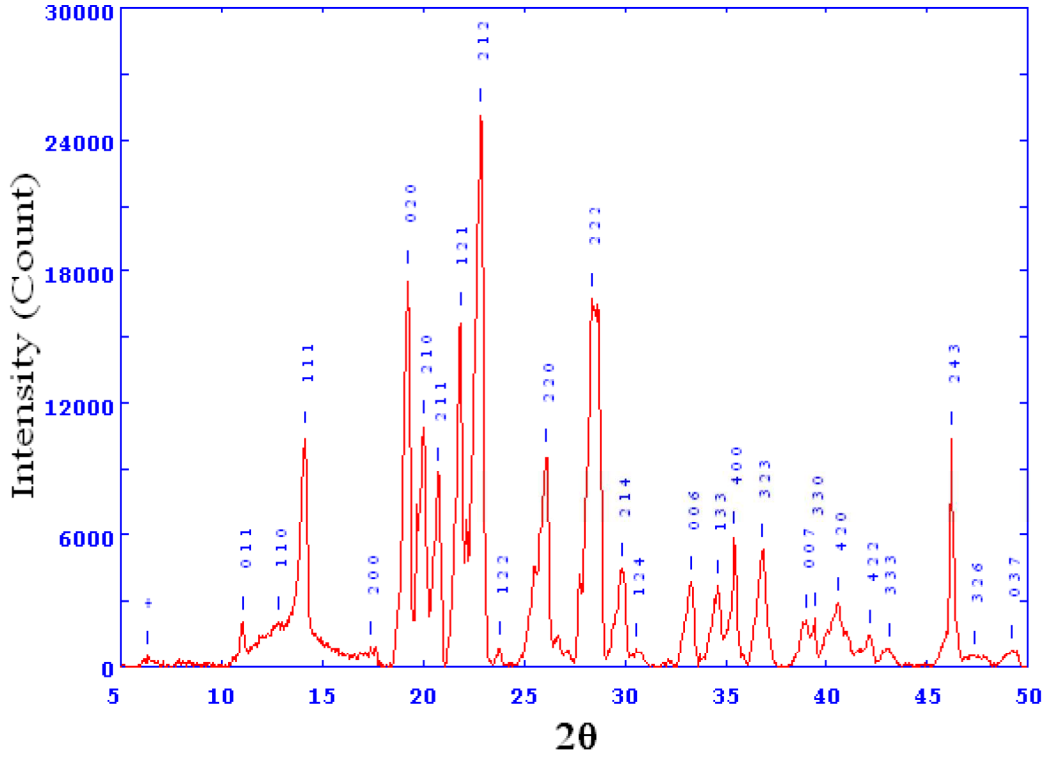


(a)

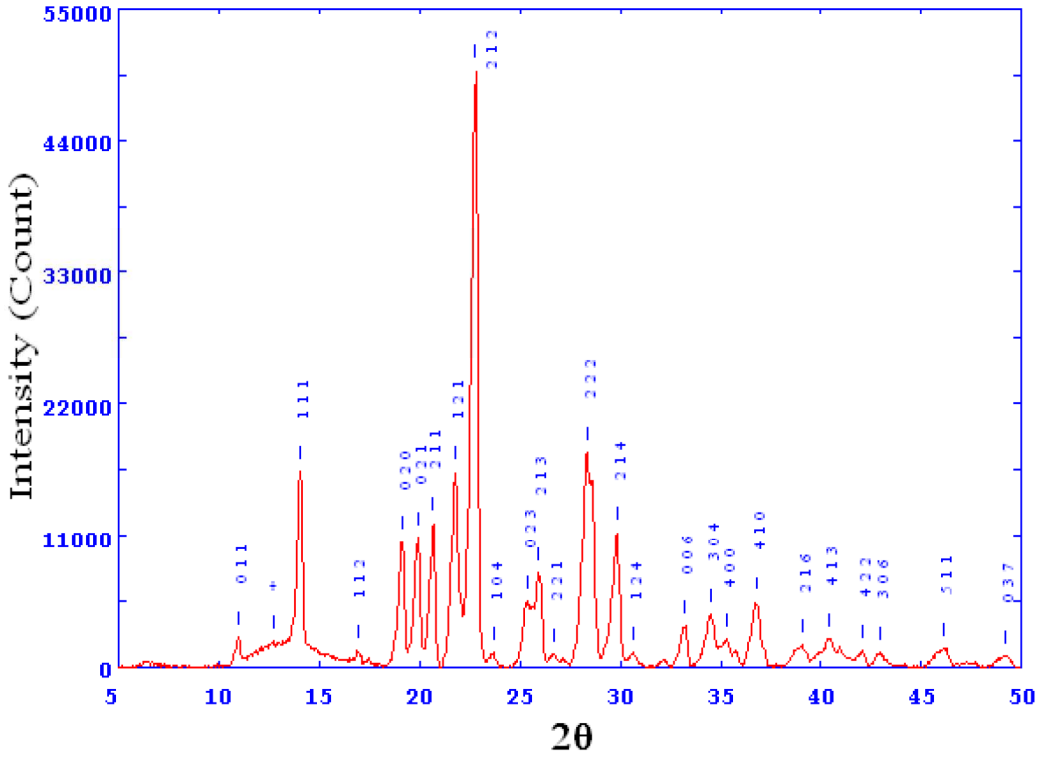


(b)

**Figure 8.16** Powder XRD data for Anilinium nitrate-I collected at RT, after heated at 383 K (a) and after reheated at 383 K (b).

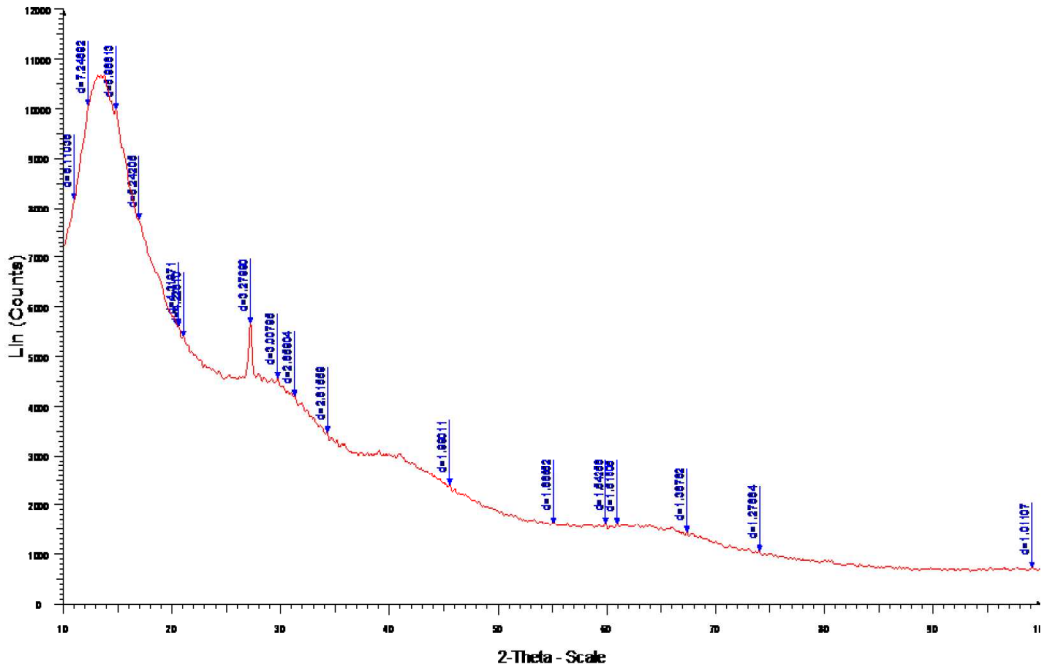


**Figure 8.17** Powder XRD pattern on white powder, obtained after drying the washed hard cocoon shaped materials in methanol at 343 K.

### 8.3.6 Structural Characterization

SEM images on anilinium nitrate-I showed that these hair-like crystals are tubes with diameters of around 10 $\mu$m, and length of 100 - 200 $\mu$m as shown in Figure 8.18 (a). These small tubes resemble bamboo shoots, as they pack above each other to give a total length of 10 - 15 cm, which looks like a bamboo tree. The presence of pores on the tubes helped us to identify the porous nature and diameter of these tubes. EDAX measurements have shown the presence of nitrogen only on the outer wall of these hallow crystals. This means the inside of the hallow tubes are hydrophobic. The SEM images on hard cocoon shaped (around 1 - 2 cm long and 0.5 cm thick) particles, resembling rosette minerals as shown in Figure 8.18 (b). In Figure 8.18 (b) right side showed SEM images for cocoon shaped material after washed with methanol and dried at 343 K. The average pore size of obtained white crystalline materials was characterized by mercury porosimetry measurements. The mercury porosimetry measurement on these materials shows that, these materials exhibit average pore diameters of 2 - 20 $\mu$m.

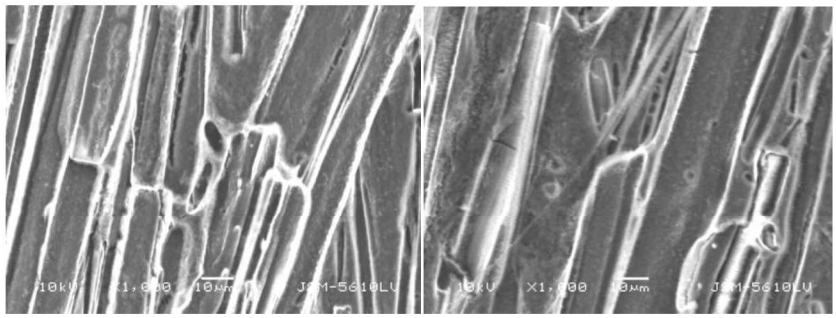

(a)

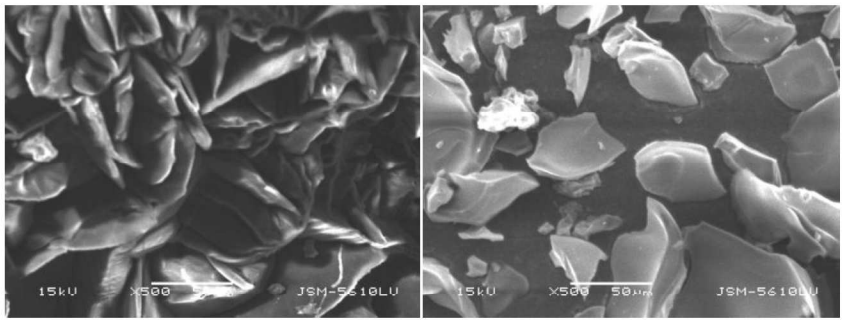

(b)

**Figure 8.18** SEM photograph showing hair-like crystal structure for anilinium nitrate-I (a), and rosette shaped porous alumina left before wash right after washed with methanol (b).

## 8.4 Conclusion

- We have successfully developed the newer way for crystal growth of organic ammonium nitrate-I salts by using the different organic amine (aromatic) and $Al(NO_3)_3.9H_2O$ in alcohol in 3:1 stoichiometric ratio. In this process we also yielded rosette shaped alumina from starting aluminium nitrate.
- TG/DTA measurement showed OANSs decomposed generally below 500 K. The decomposition of OANSs below the ammonium nitrate (decomposition temperature) followed by ignition indicates that it can used as a good explosive materials.
- Most of the OANSs are stable up to 400 K; anilinium nitrate and derivative showed mass loss around 400 K, and benzilinium nitrate and derivative above the 450 K. No constant change observed for substituent (electron withdrawing/donating) on aromatic ring for this set.
- DSC measurements showed not all OACSs have reversible solid-solid phase transition.

- Single crystal XRD suggested anilinium nitrate-II and benzilinium nitrate-II crystallized in orthorhombic space group *Pbca*, while 4-methyl anilinium nitrate-II crystallized in monoclinic space group $P2_1/c$.
- Single crystal studies on organic ammonium nitrate-II shows significant differences in N-H···O hydrogen bond present in the structure
- Powder XRD patterns of organic ammonium nitrate-I differ from organic ammonium nitrate-II.
- SEM images on hair-like crystals (anilinium nitrate-I) showed that it resemble the bamboo structure with each shot with diameters of around 10 $\mu$m, and length of 100 - 200 $\mu$m. SEM images for cocoon shaped material after washed with methanol and dried at 343 K showed that it having the pore.
- The mercury porosimetry measurement on these materials (alumina) shows it have average pore diameters of 2 - 20 $\mu$m.

## References


[1] D. C. Sorescu, D. L. Thompson, *J. Phys. Chem.* **2001**, *105*, 720-733.

[2] T. H. Goodwin, J. Whetstone, *J. Chem. Soc. abs.* **1947**, 1455-1461.

[3] G. Singh, I. P. S. Kapoor, S. M. Mannan, J. Kaur, *J. Hazad. Mater.* A **2000**, *79*, 1-18.

[4] S. R. Jain, M. V. Rao, V. R. Pai Verneker, *Proc. Indian Acad. Sci.* **1978**, *87*, 31-36.

[5] S. R. Jain, M. V. Rao, V. R. Pai Verneker, *J. Chem. Soc., Perkin Trans* **1979**, *2*, 406-410.

[6] G. Singh, I. P. S. Kapoor, S. M. Mannan, *Thermochim. Acta* **1995**, *262*, 117-127.

[7] M. K. Marchewka, A. Pietraszko, *J. Phys. Chem. Solids* **2005**, *66*, 1039-1048.

[8] T. N. Bill, T. P. Russell, *Combust. Flame* **1989**, *76*, 393-401.

[9] Y. Shinnaka, *J. Phys. Soc. Jpn.* **1959**, *14*, 1073-1083.

[10] H. C. Tang, B. H. Torrie, *J. Phys. Chem. Solids* **1977**, 38, 125-138.

[11] S. V. Baryshnikov, E. V. Charnaya, A. Y. Milinskiĭ, E. V. Stukova, C. Tien, D. Michel, *Phys. Solid State* **2010**, *52*, 392-396.

[12] **A. K. Vishwakarma**, P. Ghalsasi, P. S. Ghalsasi, *Phys. Status Solidi B* **2011**, 1-5.

[13] M. L. Ruiz, I. D. Lick, M. I. Ponzi, E. R. Castellón, A. Jiménez-López, E. N. Ponzi. *Thermochim. Acta* **2010**, *499*, 21-26.

[14] C. A. Summers, R. A. Flowers, *Protein Sci.* **2000**, *9*, 2001-2008.

[15] F. Pacholec, H. T. Butler, C. F. Poole, *Anal. Chem.* **1982**, *54*, 1938-1941.

[16] M. Dawber, I. Farnan, J. F. Scott, *Am. J. Phys.* **2003**, *71*, 819-828.

[17] Y. V. Nelyubina, K. A. Lyssenko, D. G. Golovanov, M. Y. Antipin, *Cryst. Engg. Comm.* **2007**, *9*, 991-996.

[18] M. Mylrajan, T. K. K. Srinivasan, *J. Crystallogr. Spectrosc. Res.* **1985**, *15*, 493-500.

[19] J. Bernstein, R. J. Davey and J. –O. Henck, *Angew. Chem., Int. Ed.* **1999**, *38*, 3440-3461.

[20] O. Lehmann, *Die Krystallanalyse*, Wilhelm Engelmann, Leipzig, **1981**.

[21] K. C. Hass, W. F. Schneider, A. Curioni, A. Andreoni, *Science* **1998**, *282*, 265-268.

[22] C. N. R. Rao, S. Ganguly, H. Ramachandra Swamym I. A. Oxton, *J. Chem. Soc. Faraday Trans.* **1981**, *277*, 1825-1836.

[23] H. Kraus, M. Müller, R. Prins, A. P. M. Kentgens, *J. Phys. Chem. B* **1998**, *102*, 3862-3865.

[24] I. P. S. Kapoor, M. Kapoor, G. Singh, *J. Therm. Anal. Calorim.* **2010**, *102*, 723-728.

[25] Y. Miron, *J. Hazard. Mater.* **1980**, *3*, 301-321.

[26] M. J. M. Van Oort, M. A. White, *Thermochim. Acta* **1989**, *139*, 205-217.

[27] N. Benali-Cherif, H. Boussekine, Z. Boutobba, N. Dadda, *Acta Cryst. E* **2009**, *65*, o2744.

[28] R. -J. Xu, *Acta Cryst. E* **2010**, *66*, o835.

[29] S. Gadzuric, M. Vranes, S. Dozic, *J. Chem. Eng. Data* **2010**, *55*, 1990-1993.

[30] M. Rademeyer, *Acta Cryst. E* **2003**, *59*, o1860-o1861.

[31] L. S. Reddy, S. Basavoju, V. R. Vangala, A. Nangia, *Cryst. Growth Des.* **2006**, *6(1)*, 161-173.

[32] B. W. Lucas, M. Ahtee, A. W. Hewat, *Acta Cryst. B* **1979**, *35*, 1038-1341.

[33] B. W. Lucas, M. Ahtee, A. W. Hewat, *Acta Cryst. B* **1980**, *36*, 2005-2008.

[34] C. S. Choi, J. E. Mapes, E. Prince, *Acta Cryst. B* **1972**, *24*, 1357-1361.

[35] M. Ahtee, K. J. Smolander, B. W. Lucas, A. W. Hewat, *Acta Cryst. C* **1983**, *39*, 651-655.